COMPUTER SIMULATION OF THE DROPWISE CONDENSATION PROCESS

Andrew W. Hunt

COMPUTER SIMULATION OF THE DROPWISE CONDENSATION PROCESS

by

ANDREW W. HUNT, JR.

Lieutenant, United States Navy

B.S., United States Naval Academy
(1966)

SUBMITTED IN PARTIAL FULFILLMENT

OF THE REQUIREMENTS FOR THE

DEGREE OF MASTER OF SCIENCE

IN MECHANICAL ENGINEERING

AND THE PROFESSIONAL DEGREE,

NAVAL ENGINEER

at the

MASSACHUSETTS INSTITUTE OF

TECHNOLOGY

June, 1971

COMPUTER SIMULATION OF THE DROPWISE CONDENSATION PROCESS

by

Andrew W. Hunt, Jr.

Submitted to the Department of Mechanical Engineering and to the Department of Naval Architecture and Marine Engineering in partial fulfillment of the requirements for the degree of Master of Science in Mechanical Engineering and the Professional Degree, Naval Engineer.

ABSTRACT

Using a model for the heat flux through a single drop, a computer simulation of the dropwise condensation process was carried out. For a given set of condensing conditions, the computer model predicts heat transfer coefficients and drop distributions which agree with experimental observations. Subsequently, an analysis was conducted with the model by varying the condensing parameters of site density, saturation temperature, and temperature difference. From a comparison of the analysis with experimental results, the effects of the previously mentioned parameters were determined.

Thesis Supervisor: Leon R. Glicksman

Title: Associate Professor of Mechanical Engineering

ACKNOWLEDGEMENTS

The author gratefully acknowledges assistance from the following:

Professor Leon R. Glicksman, who supervised the thesis;

my friend, Mr. Andrew H. Sims, who helped organize the coalescence routine;

my friend and colleague, Mr. Jeffrey S. Horowitz, who made suggestions which were incorporated into the model,

and Lieutenant Clark Graham, USN, who authored a comprehensive work in the field of dropwise condensation. Lt. Graham's work served as a basic reference for this thesis and provided the experiment work necessary to validate the predictions of this model.

Financial assistance from several organizations supported this study. The Naval Ship Systems Command in Washington, D. C., showed the initial interest in the thesis and provided the greatest portion of the funding. Other contributors were the Naval Architecture and Marine Engineering Department, M.I.T.; the Shell Companies Foundation, Incorporated; and the Mechanical Engineering Department, M.I.T.

TABLE OF CONTENTS

LIST OF TABLES

LIST OF FIGURES

LIST OF FIGURES
(Cont'd)

NOMENCLATURE

a = constant defined in Eq. (A.15)

A = Area (ft^2)

b = constant defined in Eq. (A.15)

c = constant defined in Eq. (A.15)

d = constant defined in Eq. (A.15)

D = drop diameter (ft)

h = heat transfer coefficient defined in Eq. (F.3) (Btu/hr ft^2 °F)

H = latent heat of vaporization (Btu/lbm)

K = thermal conductivity (Btu/hr ft°F)

M = molecular weight

Q = rate of heat transfer (Btu/hr)

r = radius of drop (ft)

R = resistance (hr °F/Btu)

$\bar{R}$ = universal gas constant

t = time or drop age (seconds)

T = temperature

v = specific volume (ft^3/lbm)

V = volume of drop (ft^3)

α = mass transfer accommodation coefficient, condensation coefficient (dimensionless)

ΔT = temperature difference (°F)

ρ = density (lbm/ft^3)

σ = surface tension (lbf/ft)

NOMENCLATURE
(Cont'd)

SUBSCRIPTS

c = curvature

cyl = cylinder

dc = drop conduction

fg = refers to change by condensation

g = vapor

i = interfacial

max = maximum

min = minimum

nuc = nucleation

s = saturation

t = total

CHAPTER I
INTRODUCTION

Over the past few decades condensers have remained essentially unchanged, while other components of the steam power plant have been improved. The potential for improvement of the condenser exists if the phenomenon of dropwise condensation can be utilized. Dropwise condensation is the process where vapor, condensing on a cold and non-wetting surface, forms liquid drops which grow and coalesce and ultimately roll off. For a surface which the liquid wets, a continuous liquid film forms and covers the surface. This latter process is called filmwise condensation and is the basis of current condenser design. Experimentally, heat transfer coefficients for dropwise condensation have been found to be an order of magnitude larger than the coefficients for filmwise condensation [1]. With this superior heat transfer property, condensers can be made smaller by weight and volume.

There are three problems retarding the use of dropwise condensation. First, there is today no well proven surface or surface coating which promotes the formation of drops. Secondly, the presence of noncondensable gases in the vapor reduces the heat transfer coefficient. There is a need for a means of reducing the noncondensables to an acceptably low limit. Finally, there is a lack of understanding of the effect of certain condensing parameters. This

study is to aid understanding by providing a theoretical prediction of the heat transfer properties of dropwise condensation by use of computer simulation of the growth and coalescence of drops from nucleation to the size at which the drops slide off the surface.

This investigation models condensation on a vertical surface. Initially the surface is bare. Then steam, without noncondensable gases, is exposed to the surface. Drops form at nucleation sites which are probably randomly distributed. They are estimated to be on the order of one hundred million sites per square centimeter [2]. The nucleation size drops are of the order of one-tenth of a micron in diameter. These small drops initially are distributed over the entire surface and begin growing very rapidly due to condensation of vapor. When neighboring drops touch, they coalesce into a single new drop. If a nucleation site is exposed by the coalescence activity, a new nucleation size drop appears. The process of growth and coalescence continues until a drop reaches a size at which the surface tension forces holding the drop on the surface are exceeded by the gravity force on the drop mass. Drops of the departing size are observed to slide down the surface and sweep other drops with them. This departing action also exposes nucleation sites.

In 1930 Schmidt, Schurig, and Sellschopp [3] first investigated dropwise condensation as a means of heat transfer. Since their investigation, there has been a controversy as to the origin of the drops and as to whether the heat is transferred through the drops or through the bare surface between the drops. The opinions can be divided into two broad theories. First, the "film theory" contends that vapor condenses on the bare surface between the drops and that the resulting liquid forms into drops. Variations of this theory are supported by the work of early investigators such as Jacob [4], Eucken [5], and Emmons [6]. More recent investigators have proposed the "nucleation theory" which disagrees with the "film theory." The proponents of the "nucleation theory" contend that drops nucleate from discrete and randomly distributed sites on the condensing surface. Furthermore, the theory states that there is no liquid between the drops and that the path of heat transfer is through the drops only. In 1935 Tammann and Boehme [7] were the first of several to observe that drops form at the same sites on successive condensation cycles. In 1964 Umur and Griffith [8] proved that there is no liquid between the drops. Using thermodynamic considerations and an optical study, they demonstrated that a film no greater than a monolayer thick could exist between the drops on the surface. Umur and Griffith's work is final strong proof of the validity of the "nucleation theory."

In agreement with the nucleation theory, Rose [9,10] was the first to develop a method of predicting the heat transfer performance of dropwise condensation by analyzing the heat transferred through a single drop and then calculating the heat flux through the condensing surface by assuming a drop distribution. By fitting four constants into his equations, Rose was able to predict values which were comparable to experimental results. Continuing with a similar approach, Graham [2], further developed an analytical expression for the heat flux through a drop which included the heat transfer resistances of drop curvature, interfacial resistance between the liquid and vapor, and conduction. In order to authenticate his model, he experimentally measured the steady state drop distribution. The smallest drops which Graham measured and counted were ten microns in diameter. Drops of smaller diameter could not be accurately observed because of a resolution limitation of the optics. The small drops are moving very fast and have diameters on the order of the wave length of visible light. By combining his experimental distribution and his analytical model, Graham found that fifty percent or more of the heat flux was transferred through drops smaller than ten microns in diameter and concluded that his heat transfer model could not be verified unless the drop distribution was known over the entire range of drop sizes. Since a complete drop

distribution cannot be experimentally determined, Graham recommended computer simulation of the dropwise condensation process as a means of obtaining the complete drop distribution.

The first computer simulation of steady state dropwise condensation was carried out by Gose, Mucciardi, and Baer [11]. The model included nucleation, drop growth due to condensation, coalescence, and removal of drops of the departing size. Their expression for drop growth from condensation considered only the conduction resistance to the heat flux through the drop. For a departing drop with a diameter of two millimeters and for a site density of 5×10^4 sites per square centimeter, their model predicted a heat transfer coefficient of approximately 460 British Thermal Units per foot square hour degree Fahrenheit.* This value is more than an order of magnitude lower than experimentally obtained coefficients.

A later study by Tanasawa and Tachibana [12] used a similar technique and predicted a coefficient of 3,700 for a site density of 4×10^3. This prediction is lower than the value of 40,000 measured by Graham [2] at the same condensing conditions. Both of the previous computer simulations modeled drops of the entire range of sizes on a fixed area. This approach and their computer facilities

*For this thesis heat transfer coefficients will have the dimensions of British Thermal Units per foot square hour degree Fahrenheit and site densities will be expressed as sites per square centimeter.

limited their investigations to artifically low site densities. Gose suggested that theoretical values would more closely match experimental results if larger site densities of 10^7 to 10^8 could be modeled. These two computer simulations and Graham's work provided the essential background for this thesis.

Using Graham's model of heat flux through a single drop, a computer simulation of the dropwise condensation process was carried out for this thesis in three parts. First, a computer model was constructed which predicts heat transfer coefficients and drop distributions for a given set of condensing conditions. Secondly, a parametric analysis was conducted varying the significant parameters, site density, saturation temperature of the vapor, and the temperature difference between the vapor and the condensing surface. The third and final part of this thesis consisted of a comparison of experimental results and model predictions.

CHAPTER II

COMPUTER SIMULATION

The Computer Model

To model a representative condensing surface of one square centimeter would require the use of approximately one hundred million nucleation sites. The computer storage necessary to identify the location and activity of these nucleation sites was not available with the IBM 360-65 Model Computer with a Fortran G Compiler used for this study. If core storage were available, the computational time for high site densities would be large and the procedure would be uneconomical. To solve the storage constraint and to build an accurate and efficient computer simulation, an innovative modeling technique was developed to model the dropwise condensation process on an initially drop free surface.

The simulation models a single cycle in which a drop of the departing size is formed on an initially bare surface. To start the modeling process, the surface is exposed to an unlimited supply of vapor. Small primary drops appear at randomly distributed nucleation sites. These drops increase their size by condensation of vapor on their surface and by coalescence with neighboring drops. As the clock time increases, the average drop size existing on the surface increases. Eventually, a drop of the departing size is

produced and slides off the surface. The simulation process stops when the first drop of departing size is formed.

The approach of the simulation is one of "viewing" the condensing surface with decreasing magnification as the average drop size on the surface increases. With a microscope one can see smaller objects by increasing the magnification, but by doing so, the field of vision is decreased. Similarly, the first area of interest is "viewed" with the highest magnification and is, therefore, the smallest area modeled. As the clock time increases, the average drop size increases. When the area of interest is no longer representative, the magnification is decreased and hence a larger area is visible. Ensuing drop growth necessitates lower and lower magnifications until departing drops are visible. An area of interest for a given magnification is called a stage. Table 1 shows how the stages are arranged for a representative calculation. Drops of the smallest size are not visible on later stages, but their presence is accounted for.

The modeling technique starts with two assumptions. The simulation models the continuous process with discrete time intervals or "time steps". Drop growth from condensation and drop coalescence are modeled to occur sequentially within the time step. Whenever the simulation clock time is increased by the time step, a routine to determine drop growth is carried out, then the coalescence activity is modeled by a

separate routine. This procedure is considered to give an accurate representation of the actual continuous process.

TABLE 1

ARRANGEMENT OF STAGES

Stage Number	Area in Square Microns	Range of Radii of "Visible" Drops in Microns
1	10^3	0.10 to 3.75
2	10^4	1.59 to 12.04
3	10^5	8.03 to 40.64
4	10^6	27.10 to 137.17
5	10^7	91.45 to 462.96
6	3.24×10^8	308.64 to 1250.00

Note: This stage arrangement is for a saturation temperature of 212°F and for a nucleation site density of 10^8 sites per square centimeter.

The growth routine determines a drop's size from an expression of drop age as a function of drop diameter. The age is increased by the time step. The drop's new size due to condensation during the time step is calculated using a relationship for drop diameter as a function of drop age. A detailed discussion of the growth routine is included in Appendix A.

Upon completion of the growth routine, a check for coalescence is carried out. The coalescence routine employed by this study is innovative and consists of a method of selectively searching for coalescences between drops and for the covering and uncovering of nucleation sites. Each drop is considered, in turn, from left to right on the stage area as the focal point of the search. A search square of two drop diameters on a side is centered on the drop of interest. Only nucleation sites and drops with centers inside the search square are considered. A determination is made whether or not the central drop blankets any of the active sites or coalesces with any of its neighbors. If an uncovered site is found to be blanketed, it is made inactive. If the drop of interest is found to be touching a neighbor drop of the same size or smaller inside the square, they coalesce to form a single new drop at the central drop's location. After the coalescence occurs, a check for the uncovering of inactive sites is made. Sites uncovered by the coalescence are made active.

The coalescence has increased the size of the central drop. Consequently, an enlarged search area must be considered so that all possible coalescences of the central drop with neighboring drops of the same size or smaller are found. After each coalescence, the search area is enlarged. When the central drop fails to coalesce, the search recommences around the next drop to the right on the stage area. When all drops have been the center of a search area, the coalescence routine ends.

The central drop only coalesces with drops of the same size or smaller. By following this procedure for all search squares, all possible coalescences are found. This search technique has the advantages of requiring a small amount of core storage and is reasonably efficient for one thousand or fewer sites per stage area. Appendix B contains a more detailed explanation of the coalescence routine.

To start the first stage requires selection of a time step value. If the time step is too large, the drops nucleated on the first time step will overlap by a large amount. Drops are observed to coalesce upon first touching. Significant overlapping is a serious departure from nature at high site densities. The time step for a given site density should be small enough to produce primary drops which do not artifically overlap.

The time step can also be too small. The problem arises because the approximation for drop radius as a function of age becomes inaccurate for very small drop radii. For this reason, the time step should be large enough to produce primary drops which are three to four times the minimum drop radius (Appendix A).

The First Stage

For a site density of 10^8, the first stage has one thousand randomly distributed nucleation sites on a square of thirty-one microns on a side. On the first time step of the first stage, the growth routine causes hemispherical drops of uniform size to appear centered on nucleation sites. The size of the uniform drops is commensurate with the time step. Next, the coalescence routine is carried out. If neighboring drops touch, they coalesce to form a single new drop centered on the nucleation site of the formerly larger drop. At the end of the coalescence routine, the drops are no longer of uniform size. Their sizes vary depending on the number of coalescences which they have undergone. The stage surface contains nucleation sites which were uncovered by the coalescence activity as well as drops of different sizes. Other nucleation sites are inactive because they are covered by a drop. Upon completion of the coalescence routine, the simulation continues by increasing the clock time by the time step.

During the second time step, new drops nucleate and grow on the nucleation sites uncovered during the previous coalescence routine. Drops already existing on the surface grow by condensation. The amount of growth depends on the drop's size and the magnitude of the time step. The coalescence check is made, and the clock is again increased. The growth and coalescence sequence with increasing time continues until the stage termination criteria is reached.

The stage termination criteria prevents "border effects". Drops near the border or edge of the stage area have an abnormally low number of neighbors; therefore, they have less opportunity to increase their size by coalescence. The effect of this unrepresentative activity is minimized by modeling drops on a given stage only until they become relatively large when compared to the surface area. There are two tests in the program for stage termination. If a single drop is formed which covers greater than ten percent of the stage area, the stage ends. A category of smaller drops may also cause termination if they cover more than twenty percent of the stage area. These drops have radii which are forty percent smaller than the radius of the single drop which can cause termination.

The amount of heat transferred through the condensing surface can be determined from the amount of liquid contained in the drops on the surface. The amount of heat transferred during a time step is simply the total

volume change of all drops on the surface multiplied by the density of the liquid and the latent heat of transformation. Since the rate of heat transfer, condensing surface area, and temperature difference between the vapor and the surface are known; the heat transfer coefficient for each time step can be calculated. From the total amount of liquid mass on the surface at a given clock time, the time averaged heat transfer coefficient for the process can be obtained and is the primary output of the stage. Figure 1 illustrates the time averaged heat transfer coefficient as a function of time.

The Second Stage

Since the area under study in the second stage is much larger than the first stage, the nucleation cannot be modeled in detail as it was on the first stage. Rather, it is assumed that on the bare area, nucleation and growth for the time interval equal to t_1 results in the same heat flux per unit area as growth of the first stage from time zero to time t_1. Thus the heat flux for the bare area is calculated as the product of bare area, time interval t_1, and average heat transfer coefficient at time t_1; see Figure 1. This heat flux results in the creation of an amount of liquid on the bare area. Drops of radius r_2 are placed on uncovered locations on the bare area to account for this amount of liquid for each time step of the second stage.

The starting conditions of the second stage are determined by an interative matching procedure which matches the results of the first stage with the start up of the second stage. The start of the second stage is at the time t_1 (see Figure 1) which is half the cycle time of the first stage. The initial drops of the second stage are assumed to be uniform in size. A drop radius, r_2, is assumed. The number of drops, N_2, is calculated so that the total amount of liquid on the surface at time t_1 is the same for the first and the second stage; this makes the average heat transfer coefficient of the first and second stage equal.

The N_2 drops are distributed on a uniformly spaced net of locations, the number of locations, N_1, being larger than N_2. At each location a random number is used to determine if a drop is present. All N_2 drops are located on the N_L locations. The N_L locations are uniformly spaced to ensure that none of the drops coalesce immediately after they are placed on the surface.

After all of the drops have been placed on the surface, the time is increased to $2t_1$ and the drops grow by condensation. Additional drops of radii r_2 are placed on uncovered locations to account for the condensing productivity of the invisible drops on the apparently bare area. The average heat transfer coefficient at time $2t_1$ is calculated and compared to the value found from the first stage. If the

values disagree, a new radius r_2 is assumed and the process is repeated until the average heat transfer coefficient of the first and second stages agree at times t_1 and $2t_1$.

When the proper value of r_2 is obtained, the second stage is allowed to proceed with time steps equal to t_1. The process of growth and coalescence of existing drops and the creation of new drops on the bare area is continued for stage two until the termination criteria is met. At this time, the third begins with a larger area and uses a starting process which is analogous to the start up of the second stage. Time steps equal one half the cycle time of the second stage are used. (Figure 2 illustrates the start up of the third stage). During the growth of the third stage, bare area is assigned an average heat transfer coefficient found from the results of the second stage for the same time interval.

Later Stages

Following stages are all similar to the third stage. They use the same effective coefficient concept and termination criteria. Each stage differs from the former by having a lower magnification and having a stage area which is ten times the larger than the previous stage area. The simulation finally ends on the last stage.

The final stage area is slightly greater than a factor of ten larger than the proceeding stage area. The size chosen is three and one quarter square centimeters and is comparable to the size of the experimental condensing

surfaces [2,13]. The termination of the last stage is different from the criteria used for the earlier stages. The last stage shuts off when a drop of the departing size is first formed. The values of the departing drop size used in this simulation were experimentally determined by Graham [2]. The final output of the complete simulation is a time averaged heat transfer coefficient for the process. The simulation program is visualized by a flow diagram, Figure 3. For the program, the input variables, source listing, and description of output are presented in Appendix C, Appendix D, and Appendix E, respectively.

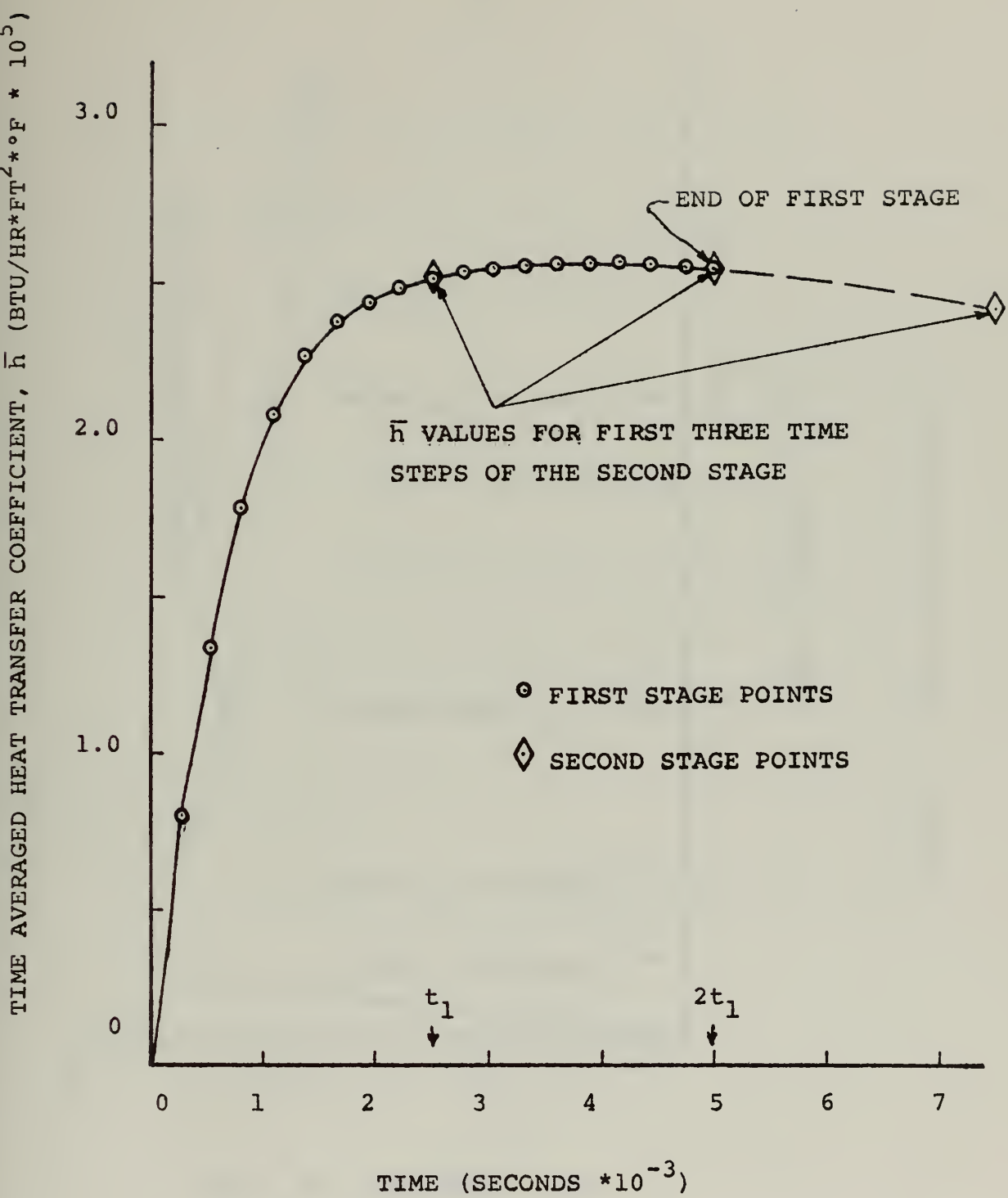

FIGURE 1 FIRST STAGE OUTPUT

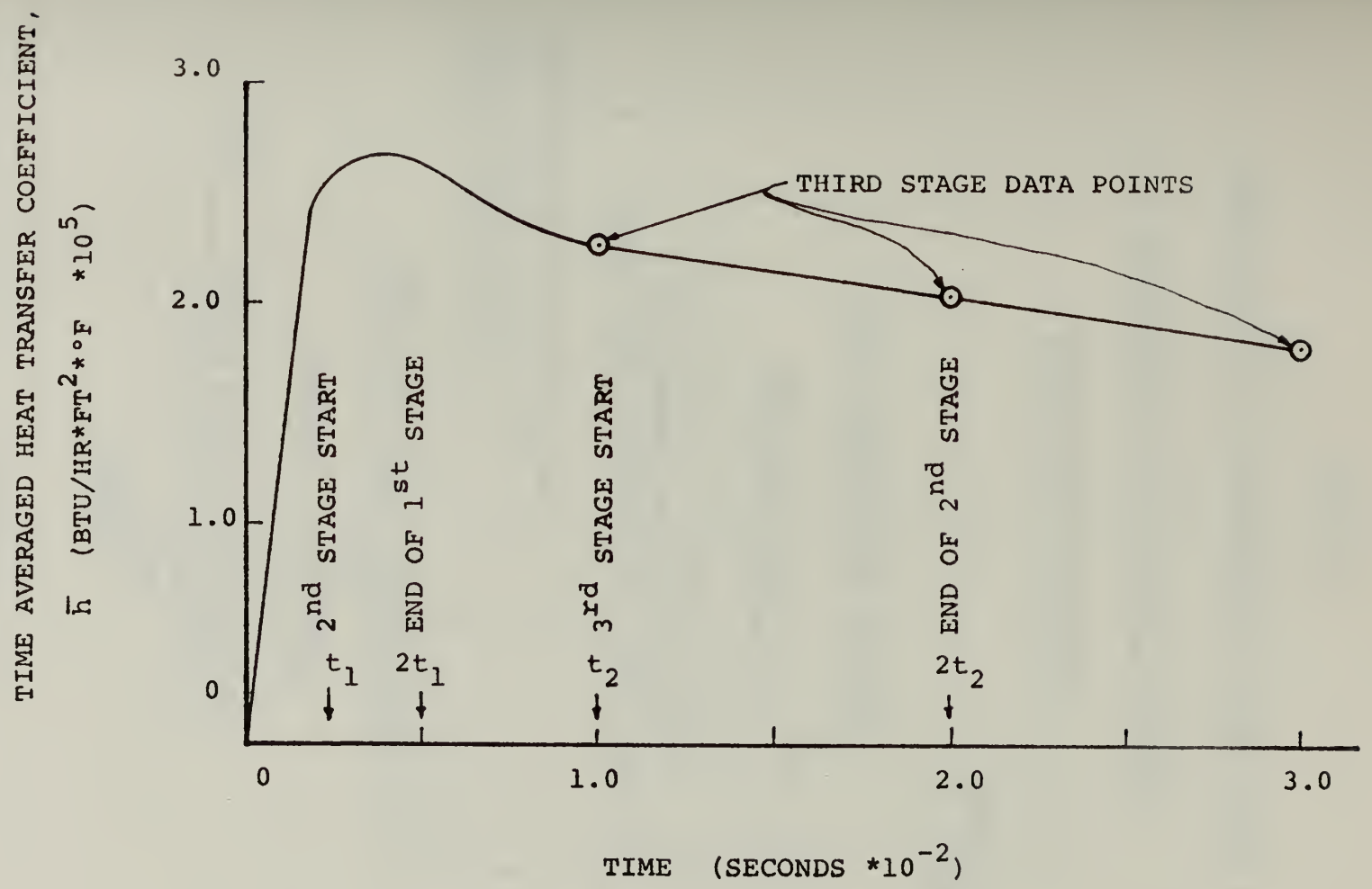

FIGURE 2 THIRD STAGE START UP

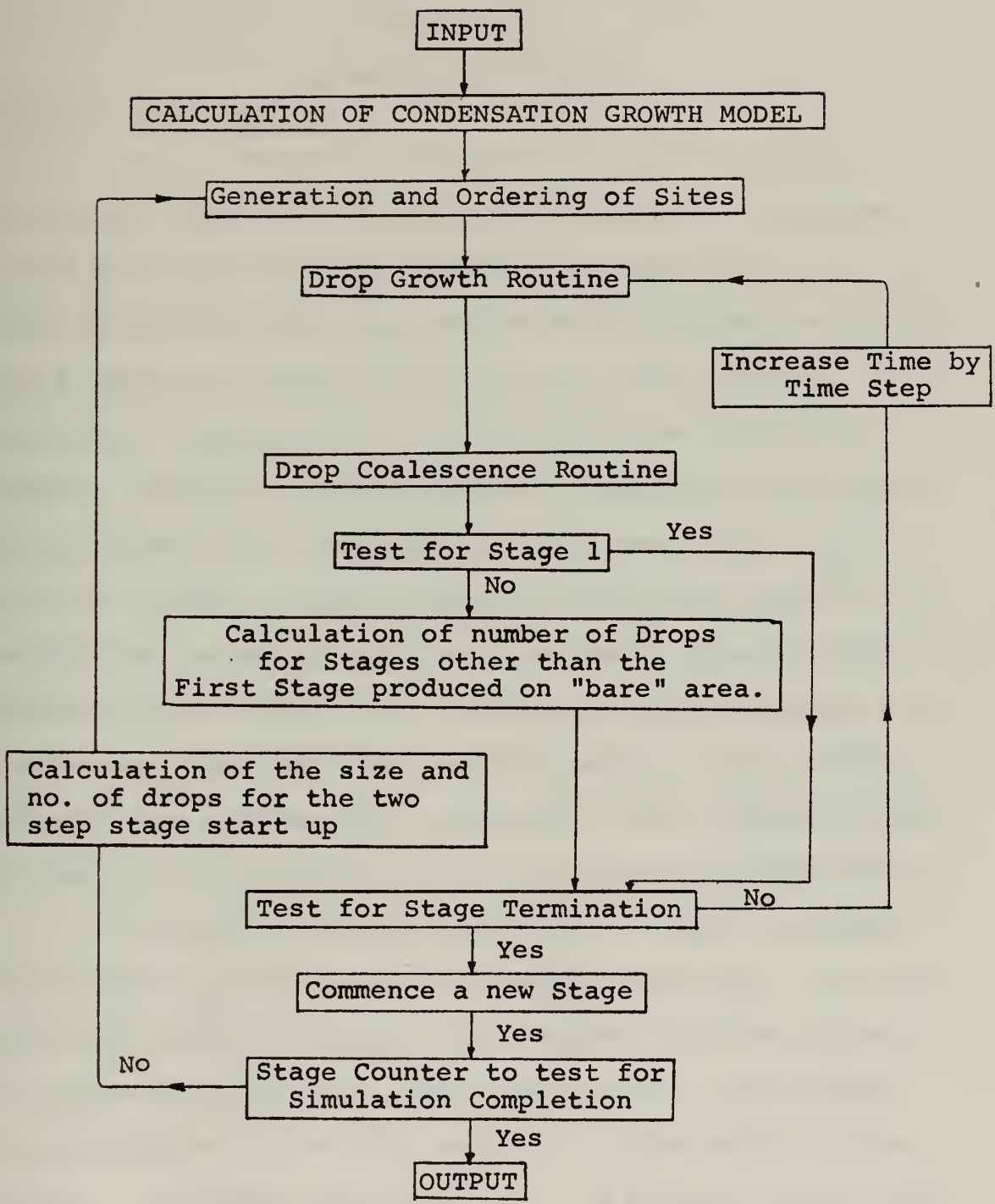

FIGURE 3

PROGRAM FLOW DIAGRAM

CHAPTER III

DISCUSSION OF RESULTS

Effect of Site Density

At a saturation temperature of 212°F and at a temperature difference of one-half degree, heat transfer predictions were made for various site densities. Figure 4 displays the time average heat transfer coefficient over a complete simulation cycle for a range of site densities. The process is controlled by two limiting factors. Initially, the surface is covered by small drops which provide little resistance to the heat flux. They limit the process of heat transfer because they are in insufficient number to provide an adequate amount of drop surface on which vapor can condense. As time increases, the average drop size increases and the amount of drop surface available for condensation increases. This effect accounts for the initial increase of the time averaged coefficient.

The heat transfer coefficient reaches a maximum where another limiting factor becomes controlling. As the average drop size increases, the average drop resistance to heat transfer increases. After the maximum, the average drop resistance becomes the controlling limitation of the process. At higher site densities, the process is initially less limited by the inadequate amount of drop surface area and becomes resistance limited more rapidly.

The higher site densities enable the process to obtain greater time averaged heat transfer coefficients.

Higher coefficient values are indicative of faster rates of mass accumulation. For this reason, drops of the departing size are produced sooner for process with higher site densities.

Once the process becomes resistance limited, the rate of decline in the time average value of the heat transfer coefficient is the same for all site densities. This observation is based on the similarity of the slopes of the curves after the maximum has been reached. The decrease in the heat transfer coefficient after the maximum appears to be independent of site density.

At the saturation temperature of 88°F and for the temperature difference of one-half degree, similar heat transfer predictions were made and are plotted on Figure 5. At the lower saturation temperature, the interfacial resistance to heat transfer is greater by an order of magnitude and has the effect of decreasing the growth rate of smaller drops by a similar amount. The reduced growth rate at lower saturation temperatures makes the process more strongly limited by the initial inadequacy of available condensing surface. Consequently, at the lower saturation temperature smaller maximums occur later in time when the site density is held constant.

A calculation of the maximum theoretical heat transfer coefficient based on a maximum drop growth rate was made. The details of the calculation are given in

Appendix F. The values obtained are plotted on Figure 6 which is a graph of the time averaged heat transfer coefficient at the end of the cycle for different site densities. The site densities examined produced coefficients well below the theoretical maximum. For a given site density, a larger value of the coefficient was obtained at the higher saturation temperature because of the faster growth rates. As the site density increases, the difference in growth rates has a more pronounced effect and the coefficient values for the two saturation temperatures diverge. As the site density decreases, the effect of the difference in growth rates diminishes and the coefficient values converge.

Next, the time averaged distribution of drop sizes over the complete cycle for various site densities were plotted and compared. Figure 7 and Figure 8 show the number of drops per square centimeter for a given drop radius at the saturation temperature of 88°F and 212°F. At either saturation temperature and for drop radii greater than ten microns, the distributions are almost invariant with site density. For radii smaller than ten microns, the distributions diverge. At the higher site densities, there are more small drops. The presence of greater numbers of small drops account for the larger heat transfer coefficients predicted at higher site densities.

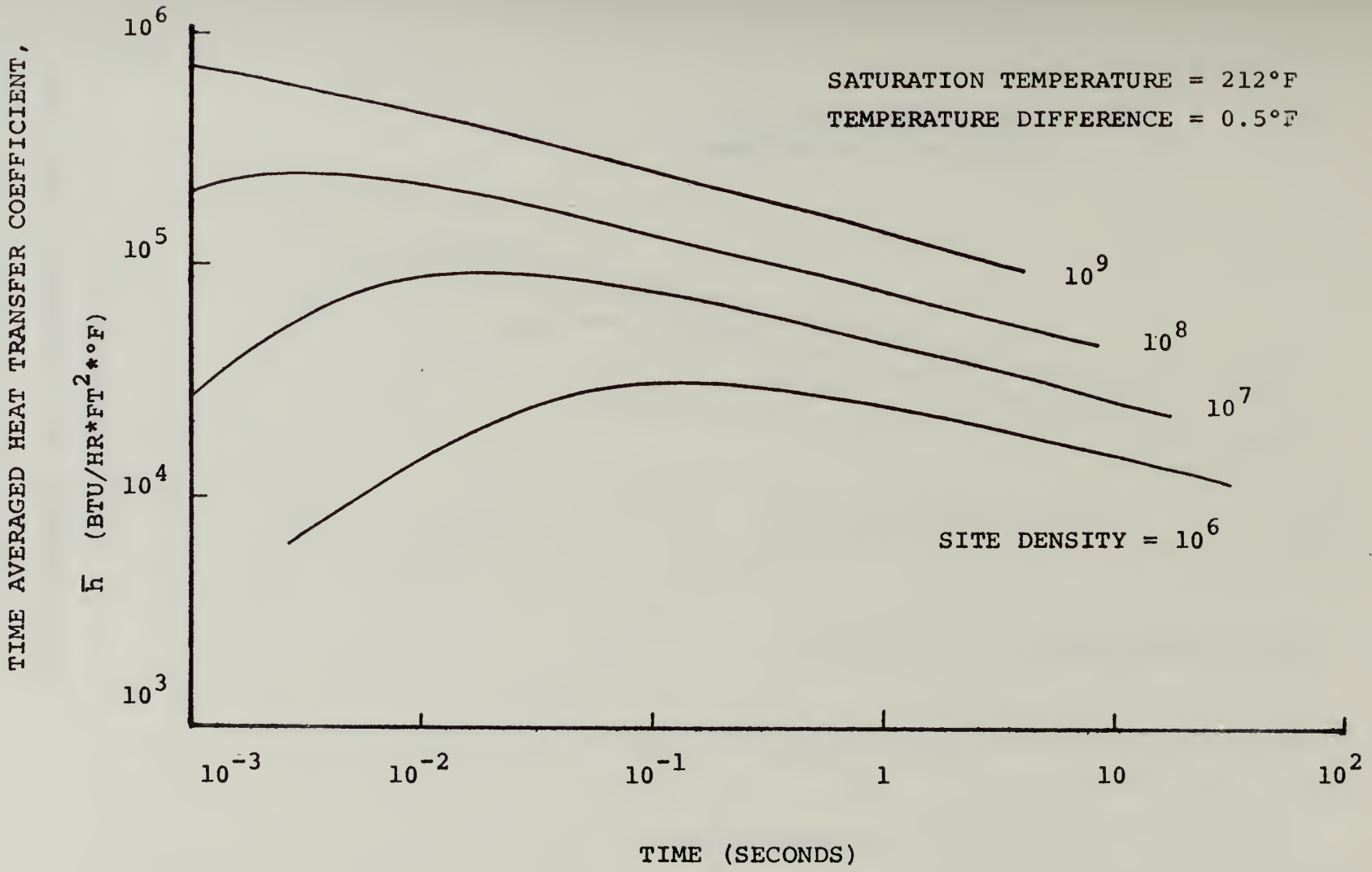

FIGURE 4 VARIATIONS OF THE TIME AVERAGED HEAT TRANSFER COEFFICIENT WITH SITE DENSITY AT 212°F

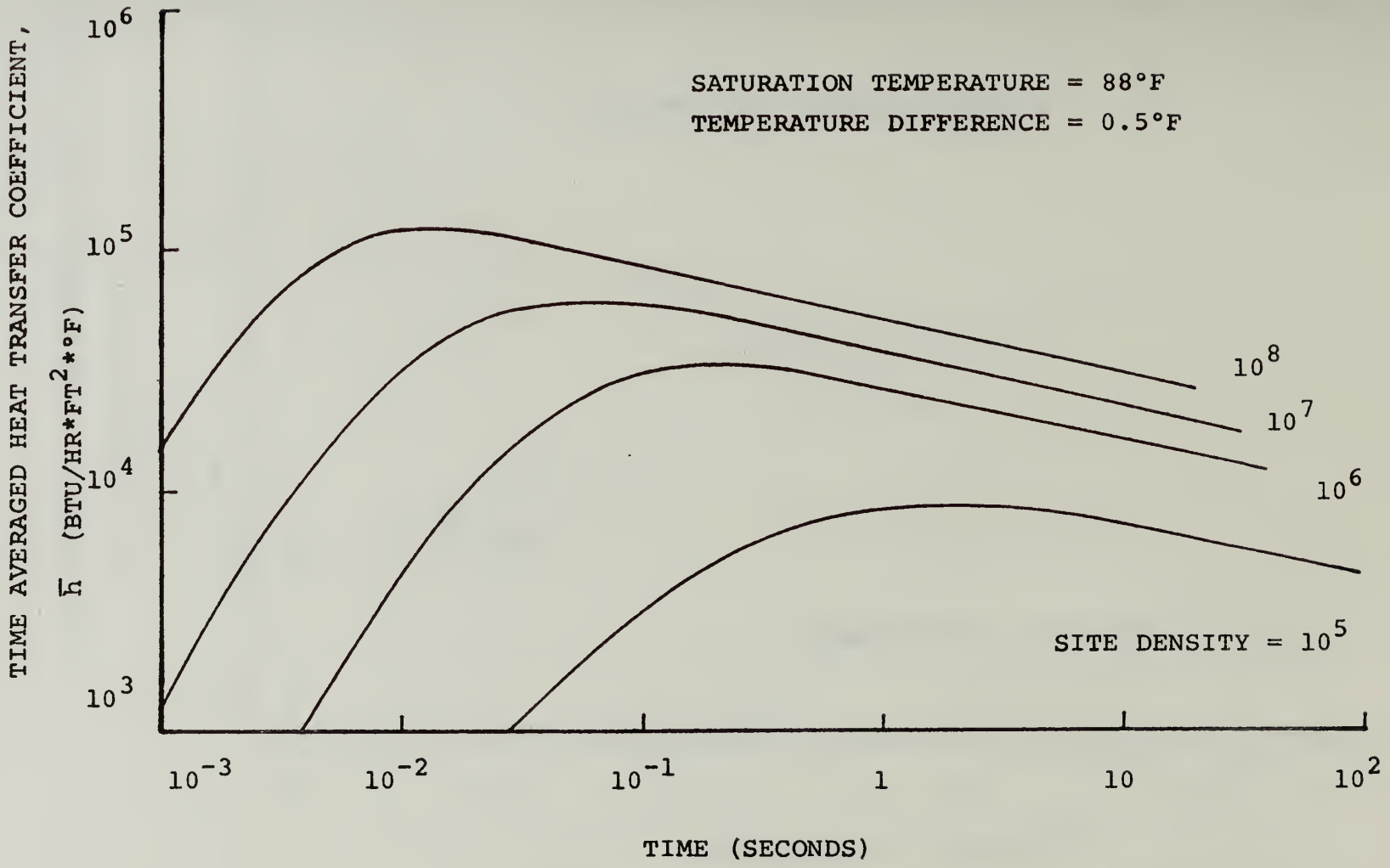

FIGURE 5 VARIATIONS OF THE TIME AVERAGED HEAT TRANSFER COEFFICIENT WITH SITE DENSITY AT 88°F

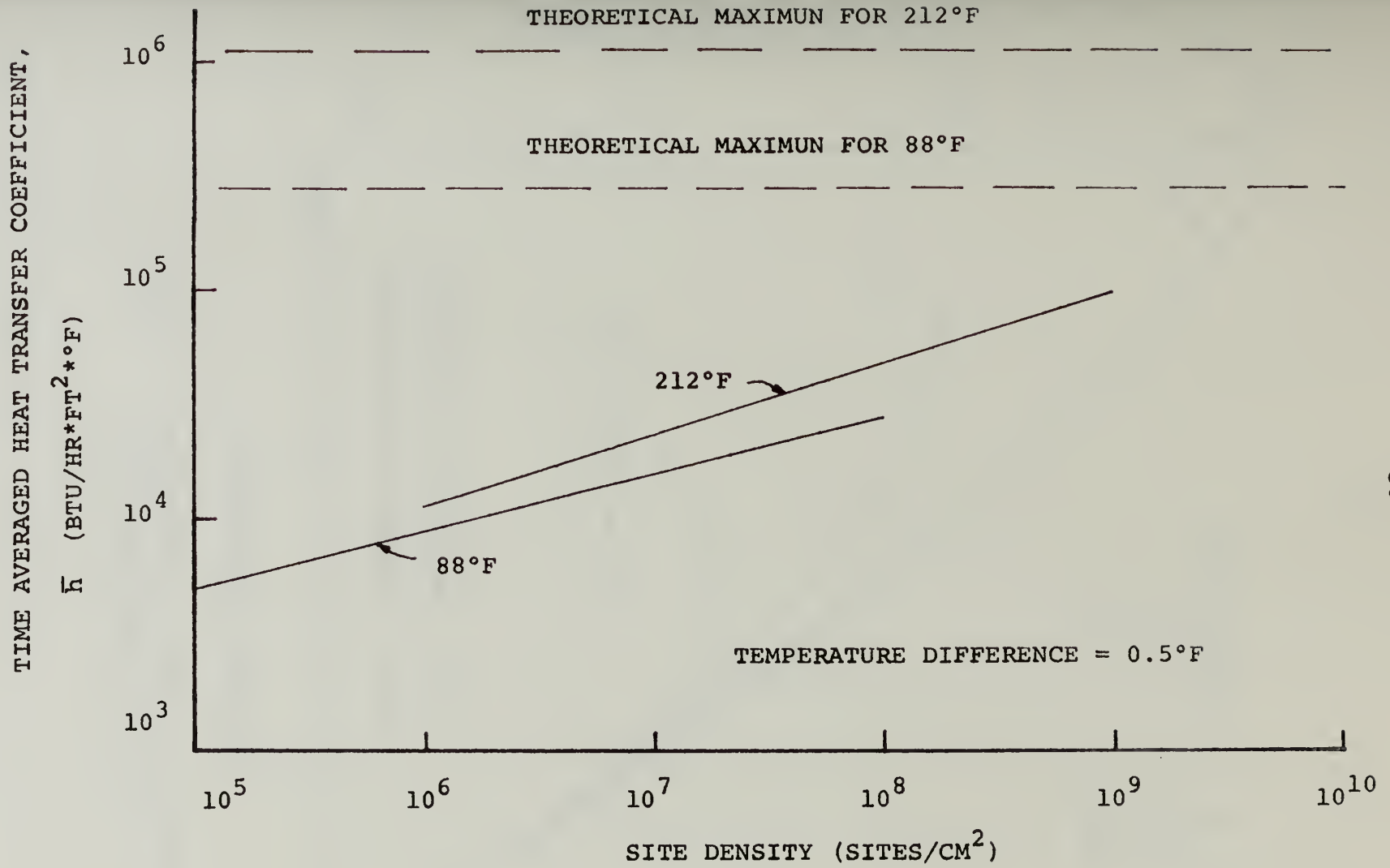

FIGURE 6 VARIATIONS OF HEAT TRANSFER COEFFICIENT WITH SITE DENSITY

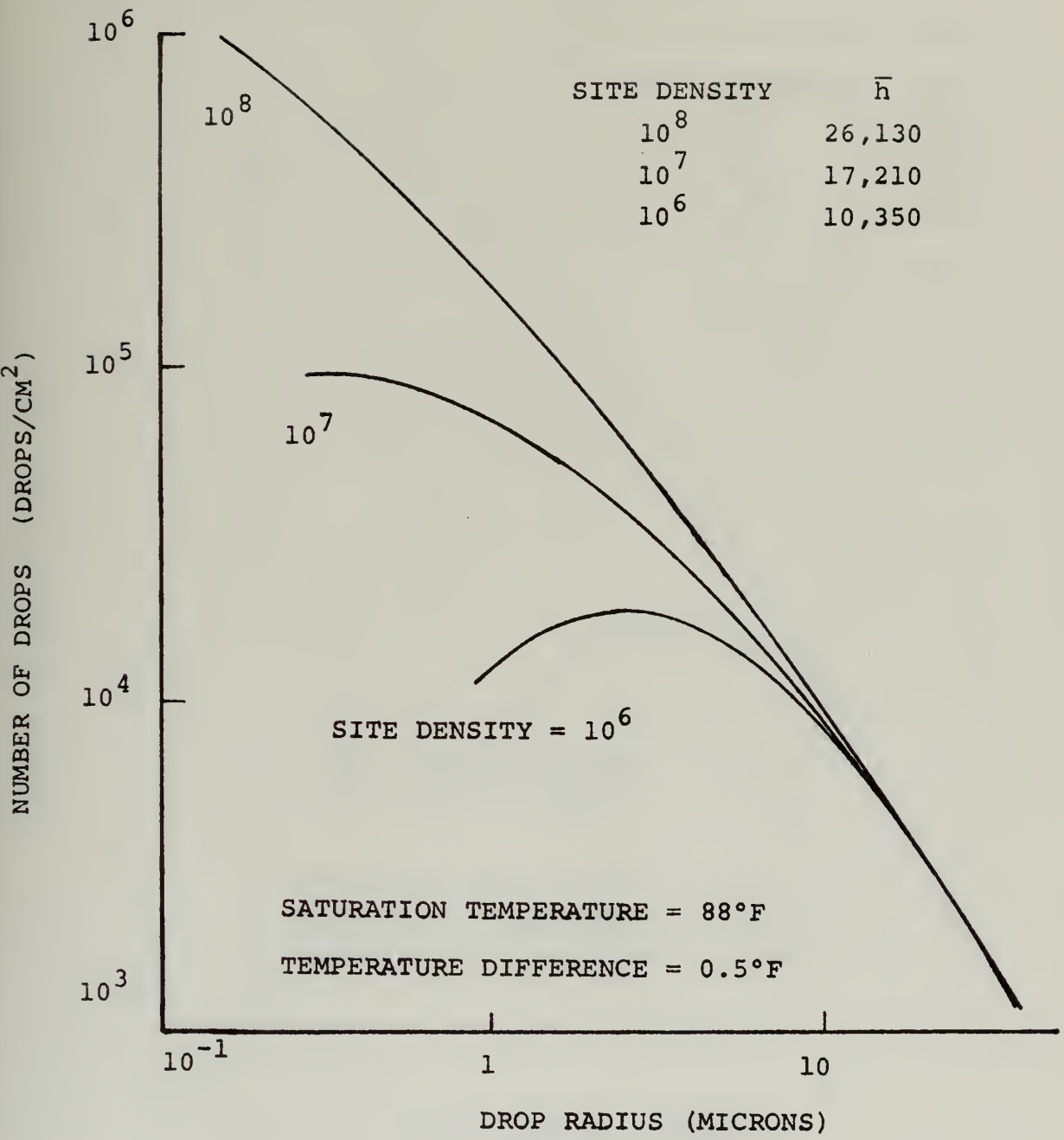

FIGURE 7 VARIATIONS OF THE DROP DISTRIBUTION WITH SITE DENSITY AT 88°F

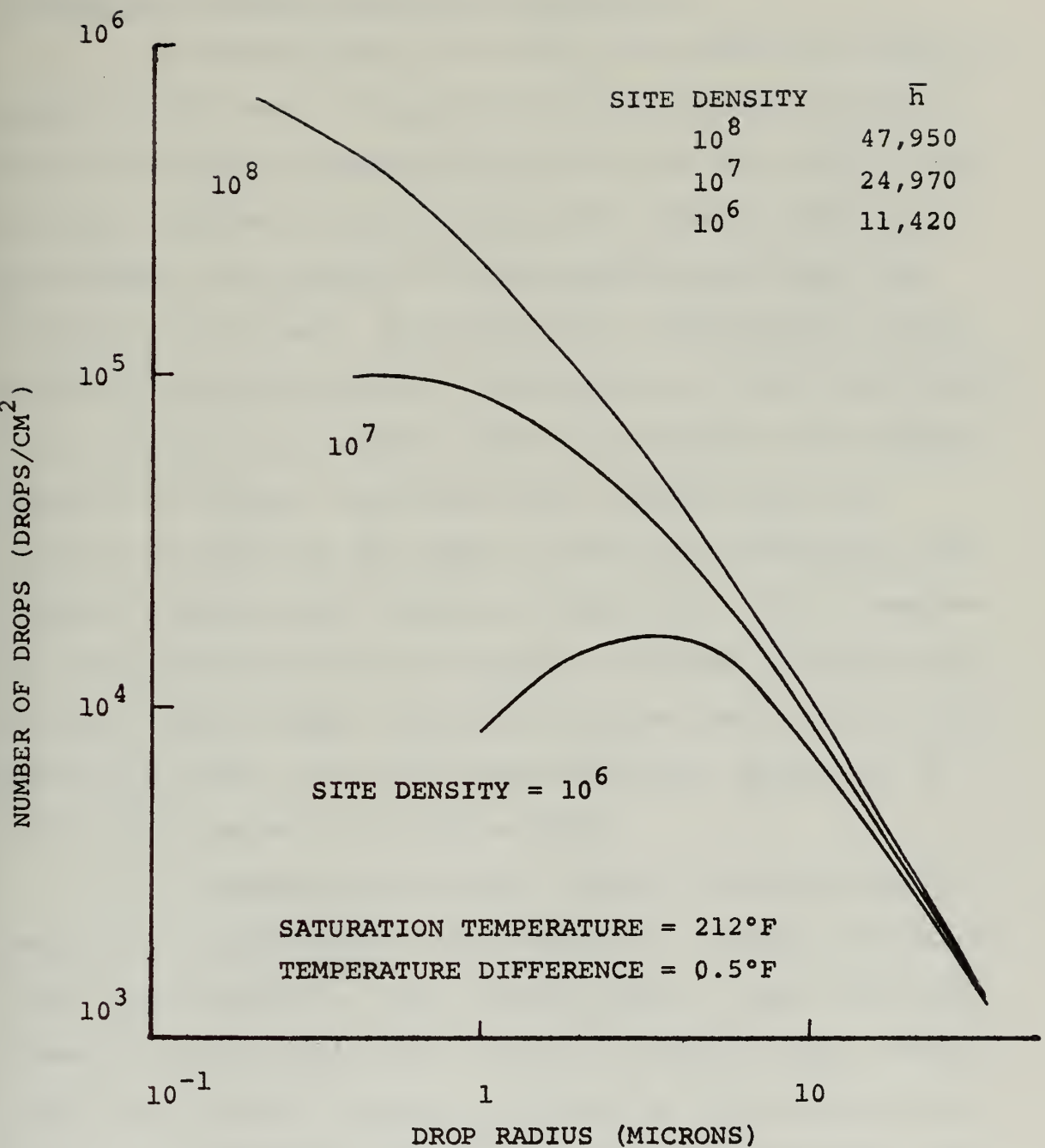

FIGURE 8 VARIATIONS OF THE DROP DISTRIBUTION WITH SITE DENSITY AT 212°F

Estimation of Experimental Site Densities

A determination of actual site density was made by comparing the model's drop distribution for the simulation cycle to Graham's measured distribution of the steady state process. Figures 9 and 10 display the model's prediction and Graham's data points for approximately the same heat transfer coefficient. The theoretical distributions agree well with Graham's measured distributions. Since the model's distributions are invariant with site density in the region measured by Graham, the actual site density had to be inferred by matching the model's predicted coefficient with Graham's measured heat transfer coefficient. For a temperature difference of one-half degree, the model indicated that Graham's smooth copper condensing surface had an active site density of about 2.5×10^7 sites per square centimeter at 212°F and of about 2.0×10^6 at 88°F.

A standard experimental method of determining site density is to photograph a portion of the condensing surface with a large number of just visible drops. These drops have diameters close to the wave length of visible light; therefore, the picture's quality is limited by the resolution of optics. By estimating the size of the drops and their number, a drop density can be calculated. The nucleation site density can be assumed to be equal to or greater than the measured drop density. The model indicated that this technique may yield an incorrect estimate at high site

densities. For various nucleation site densities of the model, Table 2 shows the model's highest instantaneous drop density for different radii. Even if drops with a radius of one micron could be accurately measured, the nucleation site density could not with certainty be inferred.

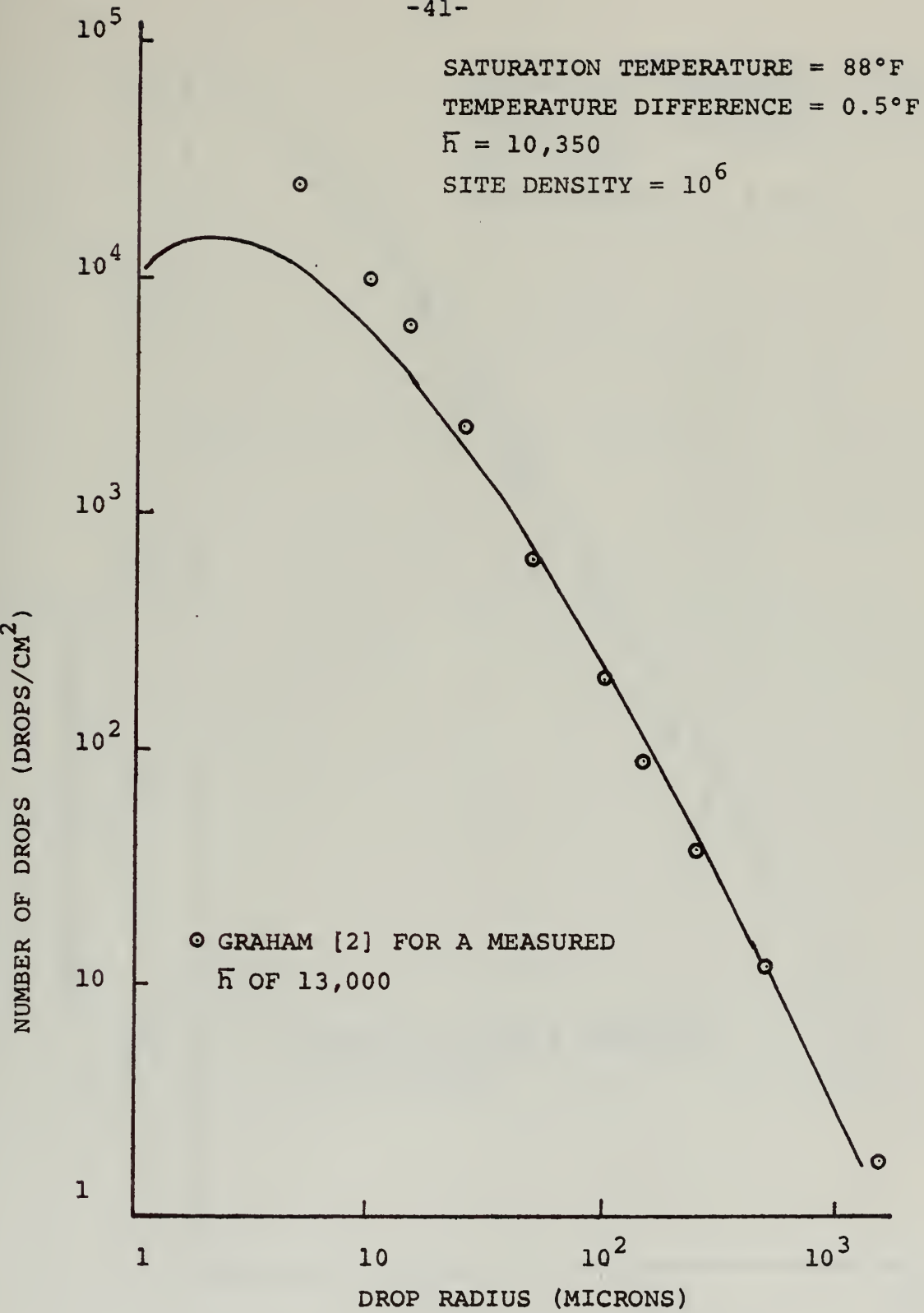

FIGURE 9 COMPARISON OF PREDICTED AND MEASURED DROP DISTRIBUTIONS AT 88°F

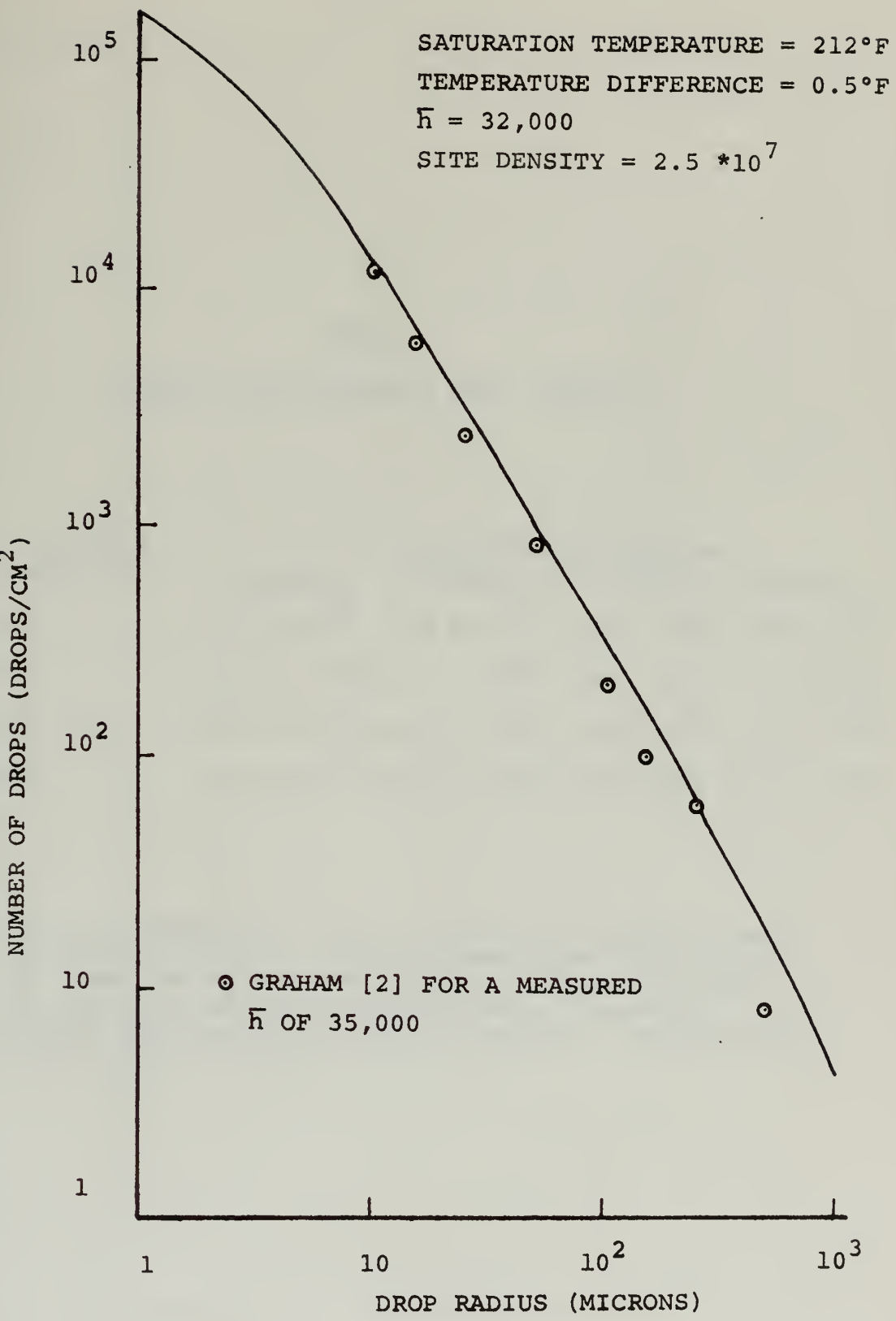

FIGURE 10 COMPARISON OF PREDICTED AND MEASURED DROP DISTRIBUTIONS AT 212°F

TABLE 2

HIGHEST INSTANTANEOUS DROP DENSITY

Model's Nucleation Site Density	Drop Radius in Microns 1.0	2.5	5.0	10.0
10^6	8.1×10^5	7.4×10^5	3.6×10^5	9.0×10^4
10^7	3.6×10^6	1.4×10^6	3.3×10^5	6.0×10^4
10^8	7.6×10^6	2.3×10^6	2.2×10^5	9.0×10^4
10^9	1.0×10^7	2.0×10^6	3.7×10^5	8.0×10^4

Note: The site densities are in dimensions of sites per square centimeter. The drop densities have units of drops per square centimeter. The predictions are for the condensing conditions of one-half degree temperature difference and for a saturation temperature of 212°F.

Effect of Temperature Differences

At the saturation temperature of 88°F and 212°F and for the site densities determined by matching Graham's measured heat transfer coefficients, predictions were made for various temperature differences between the vapor and the surface. The results are displayed in Figure 11 and Figure 12. The model predicts an approximately constant heat transfer coefficient for a constant site density in the temperature difference range from a quarter degree to four degrees. The experimental results also plotted on the figures agree with the constant heat transfer coefficients values for temperature differences greater than one degree. Below one degree the heat transfer coefficients are experimentally observed to decrease. This disagreement between the model prediction for low temperature difference may be attributable to the model's assumption of constant site density.

The minimum drop radius increases rapidly as the temperature difference is reduced. Figure 13 is a graph of the minimum drop radius plotted as a function of temperature difference. The curve indicates that as the temperature difference decreases from one degree to a quarter degree, the minimum drop radius increases by a factor of five for both 88°F and 212°F saturation temperatures. At high site densities, large values of the minimum radius could cause artificial overlapping on the first stage of the model and

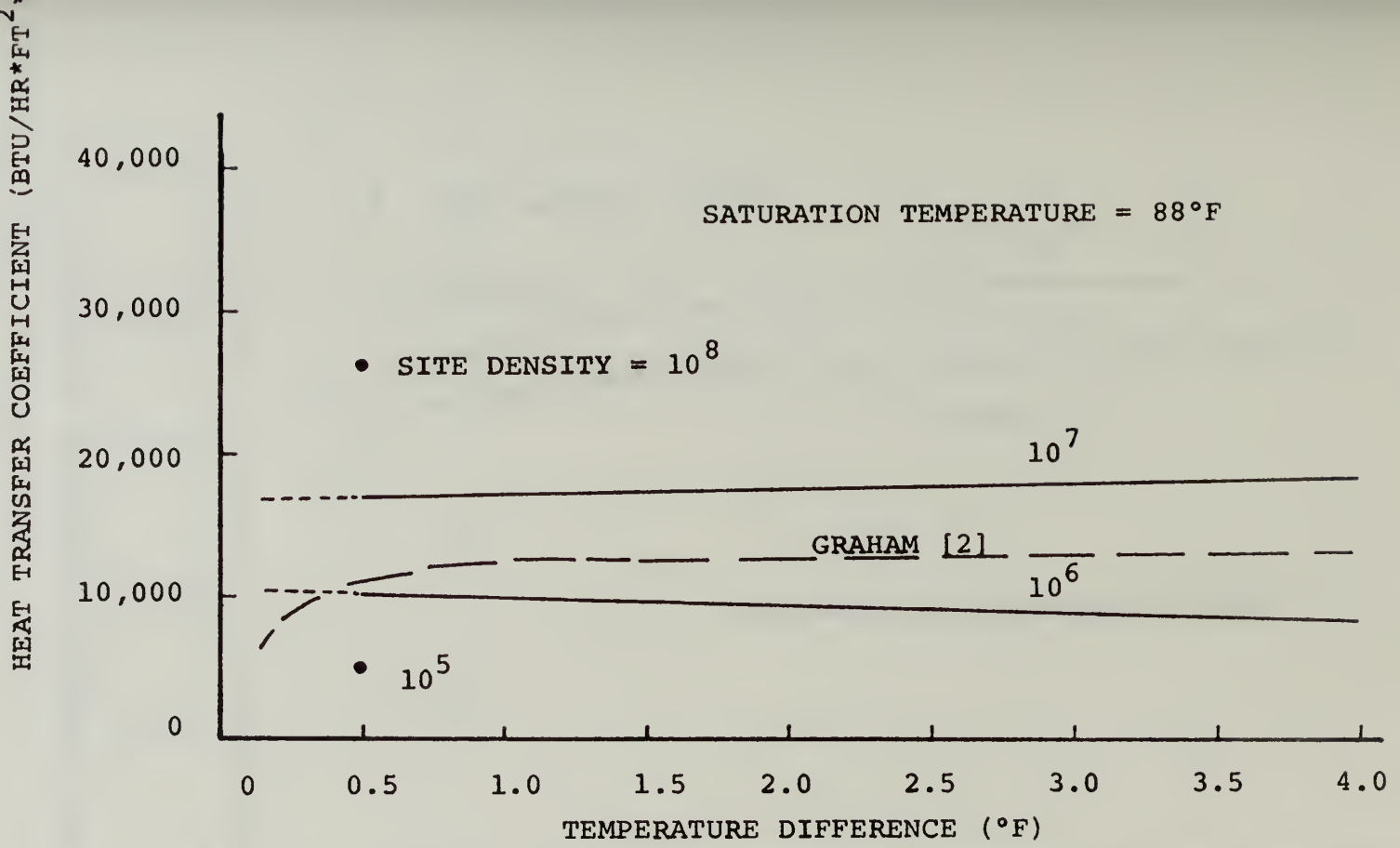

FIGURE 11 VARIATIONS OF THE HEAT TRANSFER COEFFICIENT TEMPERATURE DIFFERENCE AT 88°F

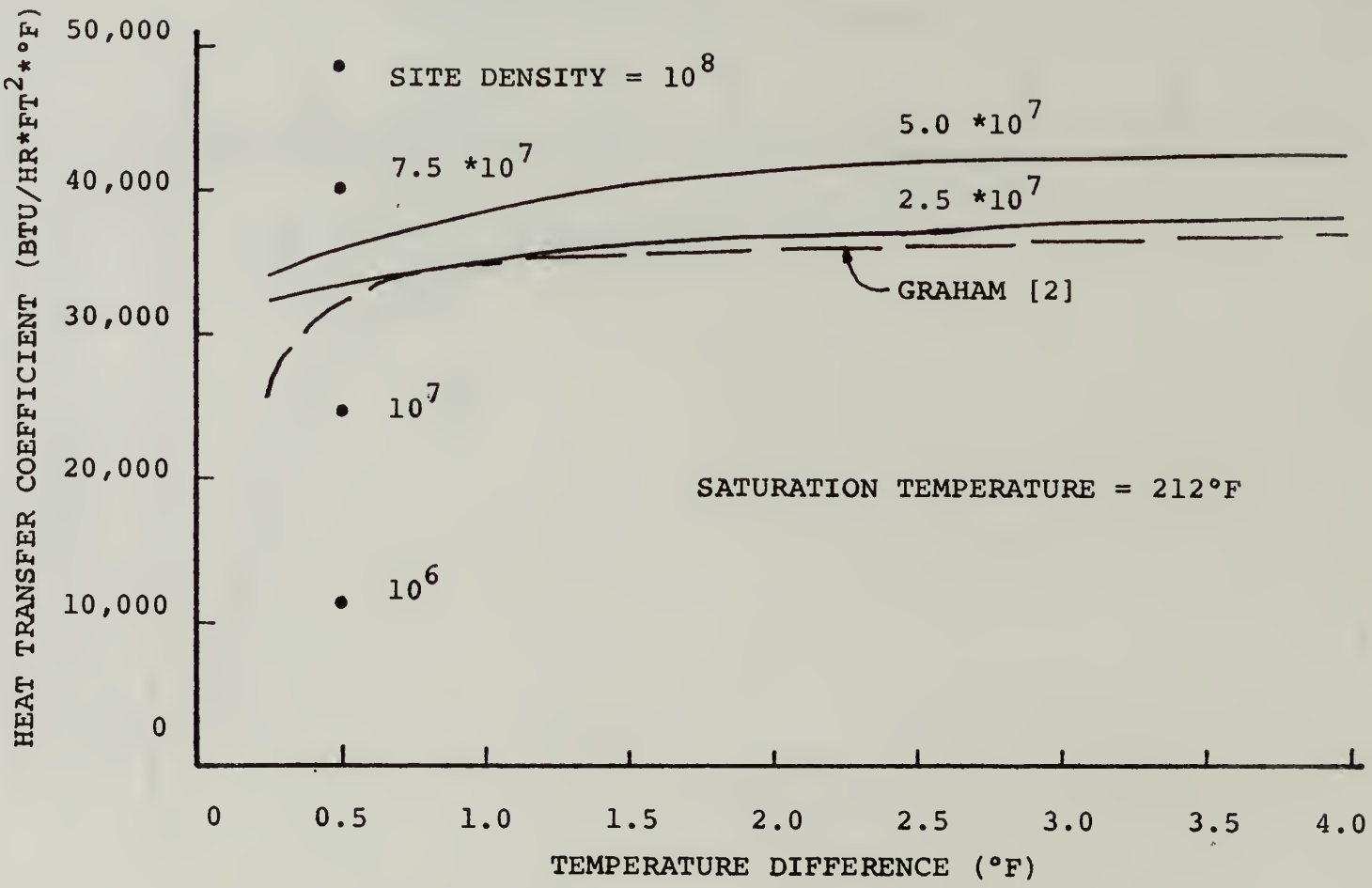

FIGURE 12 VARIATIONS OF THE HEAT TRANSFER COEFFICIENT WITH TEMPERATURE DIFFERENCE AT 212°F

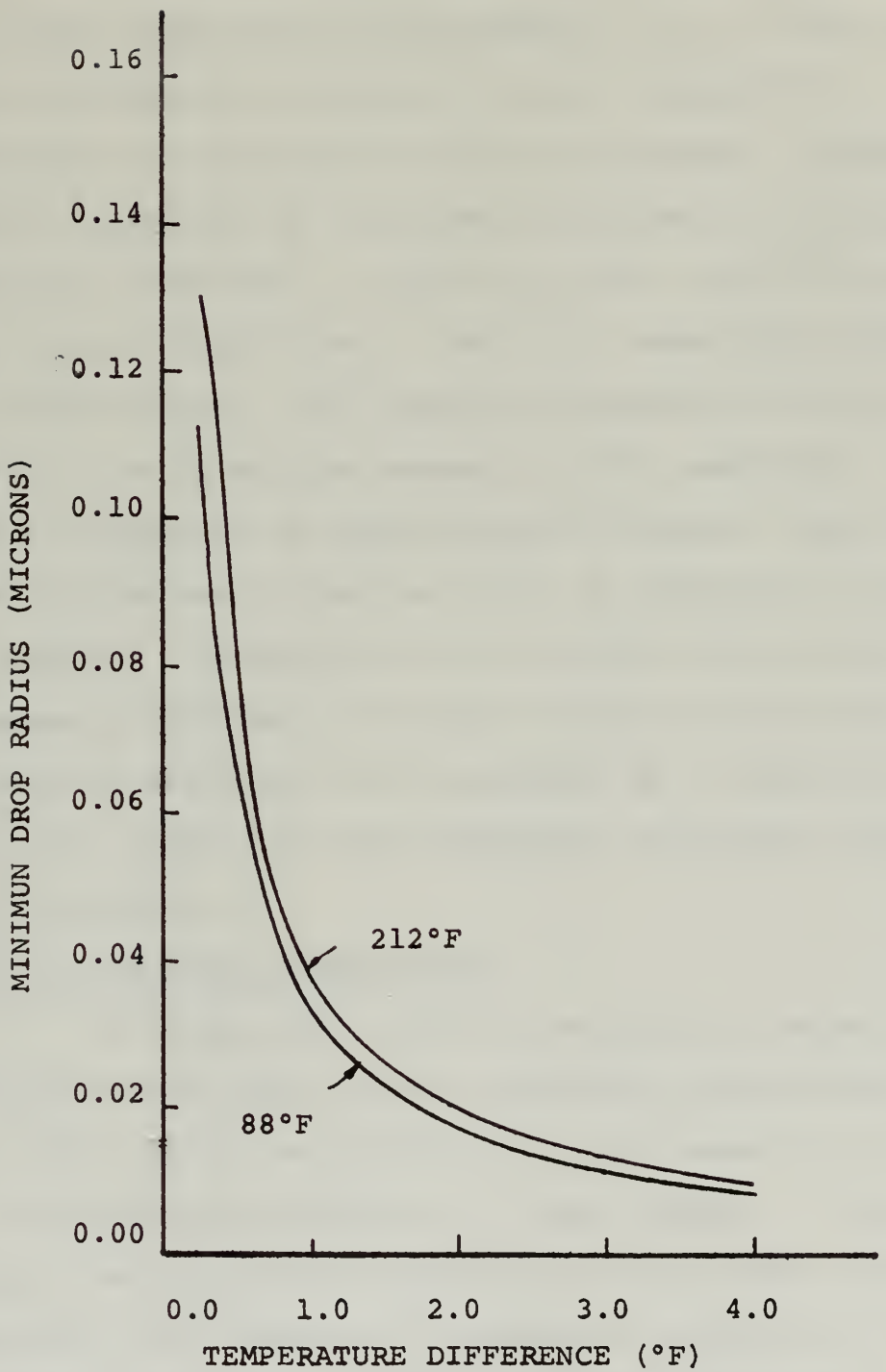

FIGURE 13 VARIATIONS OF MINIMUN DROP RADIUS WITH TEMPERATURE

thereby predict an erroneously high heat transfer coefficient.

The maximum theoretical site density for a given temperature difference was determined to see if the constant site density assumption at small temperature differences was causing artificial overlapping. Appendix G contains derivation of a maximum site density for a given temperature difference. Figure 14 is the result of a calculation using the derivation. Even for a temperature difference of a quarter degree, the theoretical maximum density is well above the site densities assumed for this analysis. The model's predictions at temperature differences less than one degree are believed to be valid for an assumption of constant site density. Kinematics of drop growth cannot account for the measured decrease in the heat transfer coefficient. The observed decrease can be explained by a reduction in the actual site density as the temperature difference decreases below one degree.

Effect of Saturation Temperature

To isolate the effect of saturation temperature, calculations were made for the saturation temperatures of 88°F, 150°F, 212°F, and 274°F at the site density of 10^7 and at the temperature difference of three degrees. Figure 15 displays the theoretical prediction for the heat transfer coefficient as a function of saturation temperature at the constant site density. Above 150°F the coefficient remains

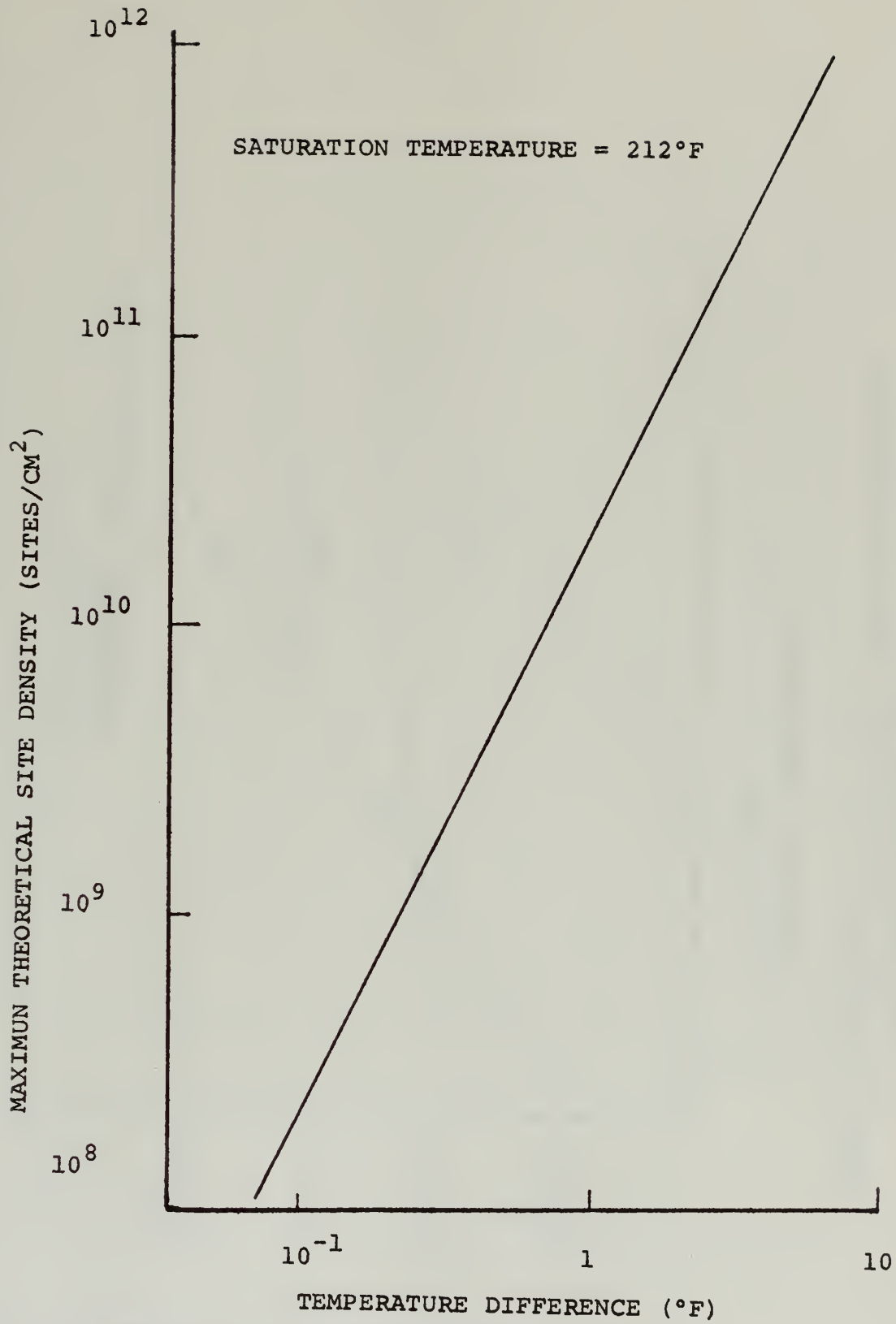

FIGURE 14 MAXIMUN THEORETICAL SITE DENSITY AT 212°F

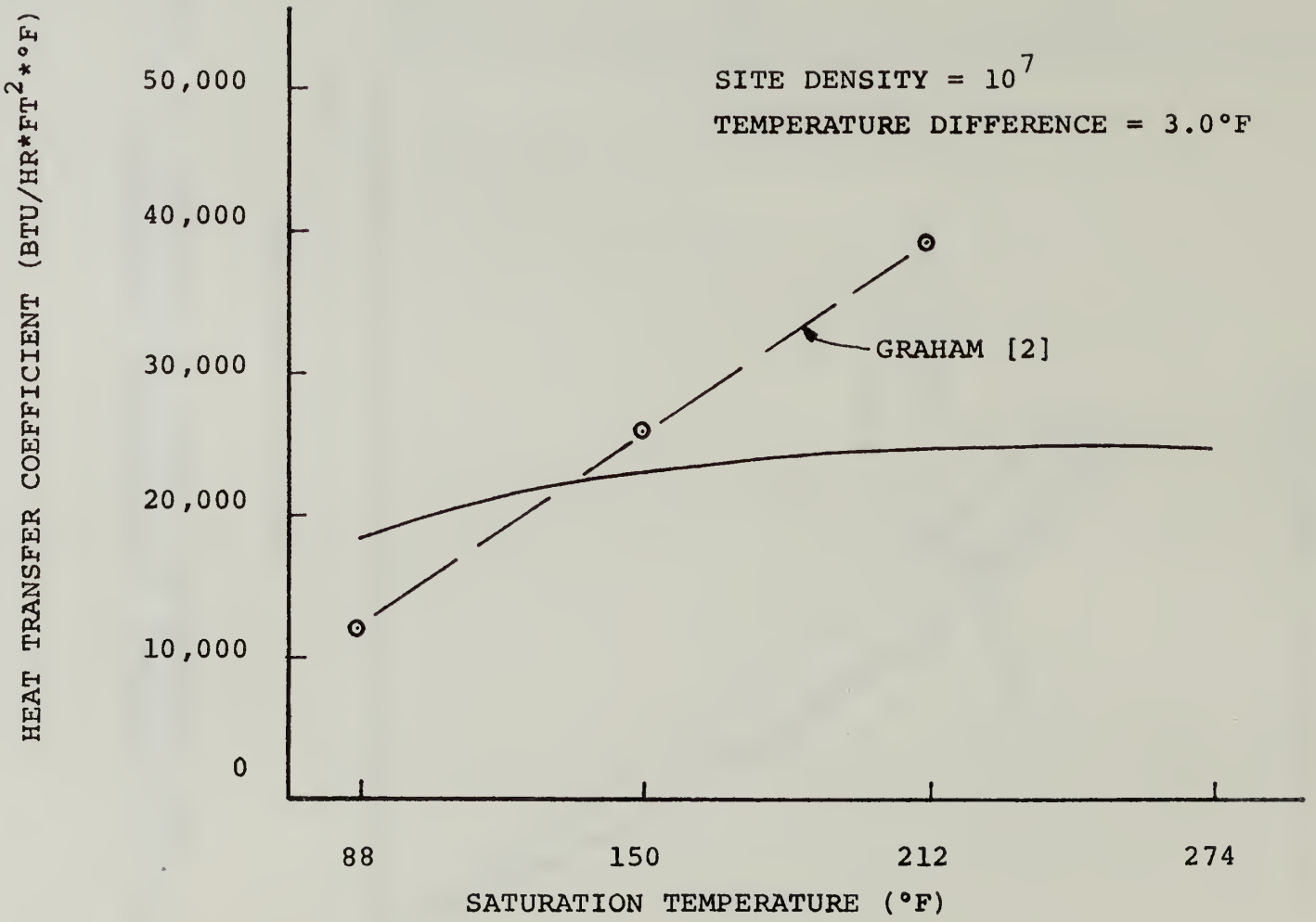

FIGURE 15 VARIATIONS OF THE HEAT TRANSFER COEFFICIENT WITH SATURATION TEMPERATURE AT CONSTANT SITE DENSITY

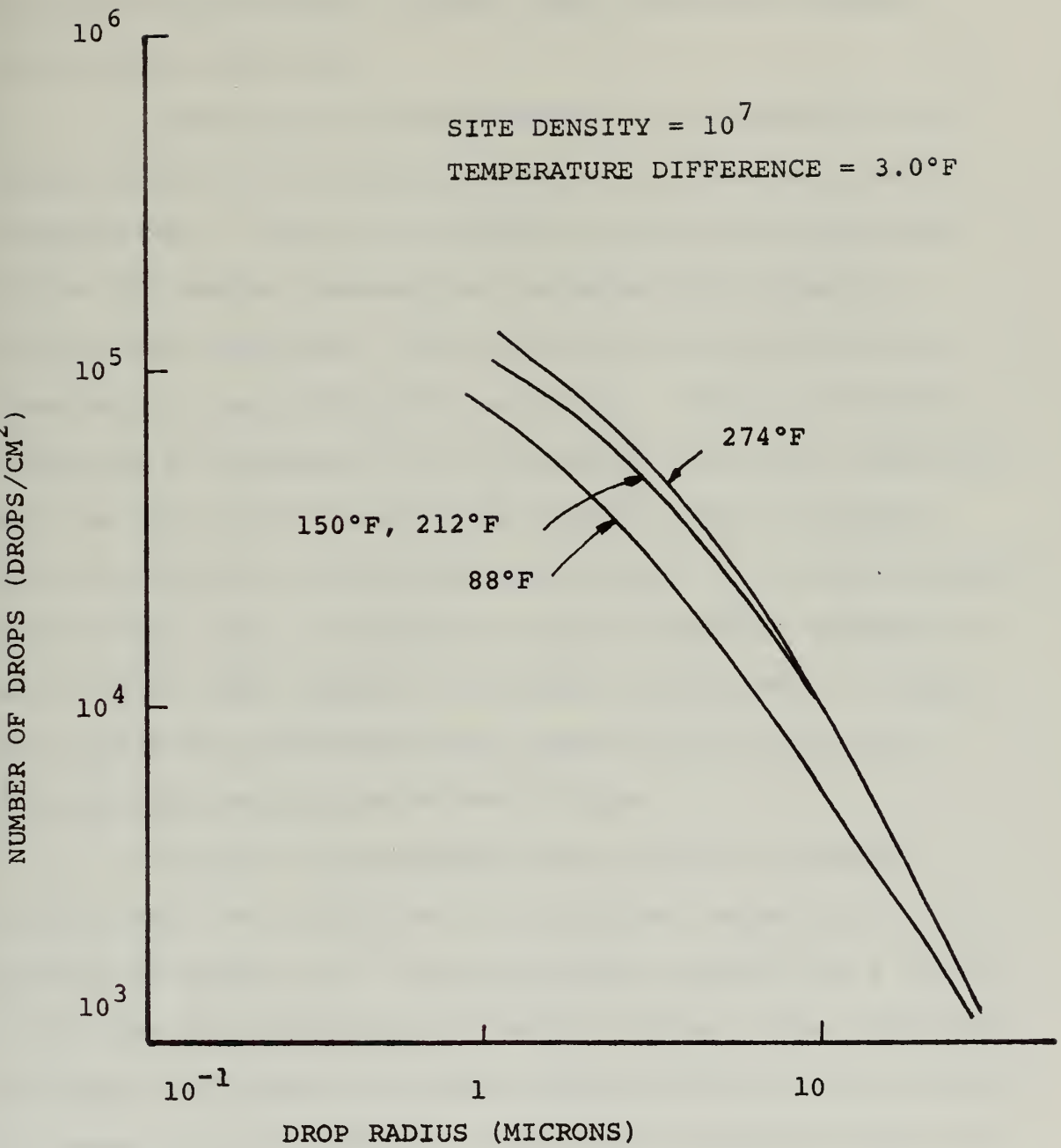

FIGURE 16 VARIATIONS OF THE DROP DISTRIBUTION WITH SATURATION TEMPERATURE AT CONSTANT SITE DENSITY

approximately constant. Below 150°F the heat transfer coefficient decreases.

The cause of the decrease can be understood by examining the drop distributions for the four saturation temperatures. Figure 16 displays the drop distributions. As the saturation temperature increases, the number of small drops increases. This effect can be explained by considering the interfacial resistance. As the saturation temperature increases, the interfacial resistance decreases; and the drop growth rate of the smaller drops increases. For the constant site density assumption, it is the increased growth rate that is responsible for the greater numbers of small drops which appear in the drop distribution. Higher heat transfer coefficients are predicted when the drop distribution contains more small drops.

Graham's experimental data for heat transfer coefficients as a function of saturation temperature is also plotted on Figure 15. The experimental result has a greater slope than the constant site density curve. This difference of slopes is further indication that the actual site density decreases as the saturation temperature decreases from 212°F to 88°F.

Time Necessary to Produce a Drop of the Departing Size

At a saturation temperature of 212°F and for a temperature difference of two degrees, predictions were made by varying site density in order to match Westwater's data [13]

for heat transfer coefficients and sweeping frequency of drops of the maximum size. The frequencies were converted into the time necessary to produce a drop of the departing size. Figure 17 shows measured and predicted heat transfer coefficients plotted as a function of the time necessary to produce departing drops. For the same heat transfer coefficient, the model predicts times which are twice as large as Westwater observed. Figure 18 shows the model's time averaged coefficient as a function of simulation time at the same condensity conditions. Reducing the model's cycle time by a factor of two means only a twenty percent increase in the model's predicted coefficient. For this reason, the lack of agreement with measured times is not considered to invalidate the other results of the model.

This disagreement may be attributed to the hemispherical drop assumption or to the model's failure to account for sweeping. Drops of all sizes were assumed to be hemispherical in shape. A flatten or distorted drop of the same volume as a hemispherical drop will cover a larger portion of the surface. The larger surface coverage for the same drop mass implies a greater opportunity for coalescence. Since large drops grow mostly by coalescence [2,11], the distorted drops should mature faster than the perfectly hemispherical drops.

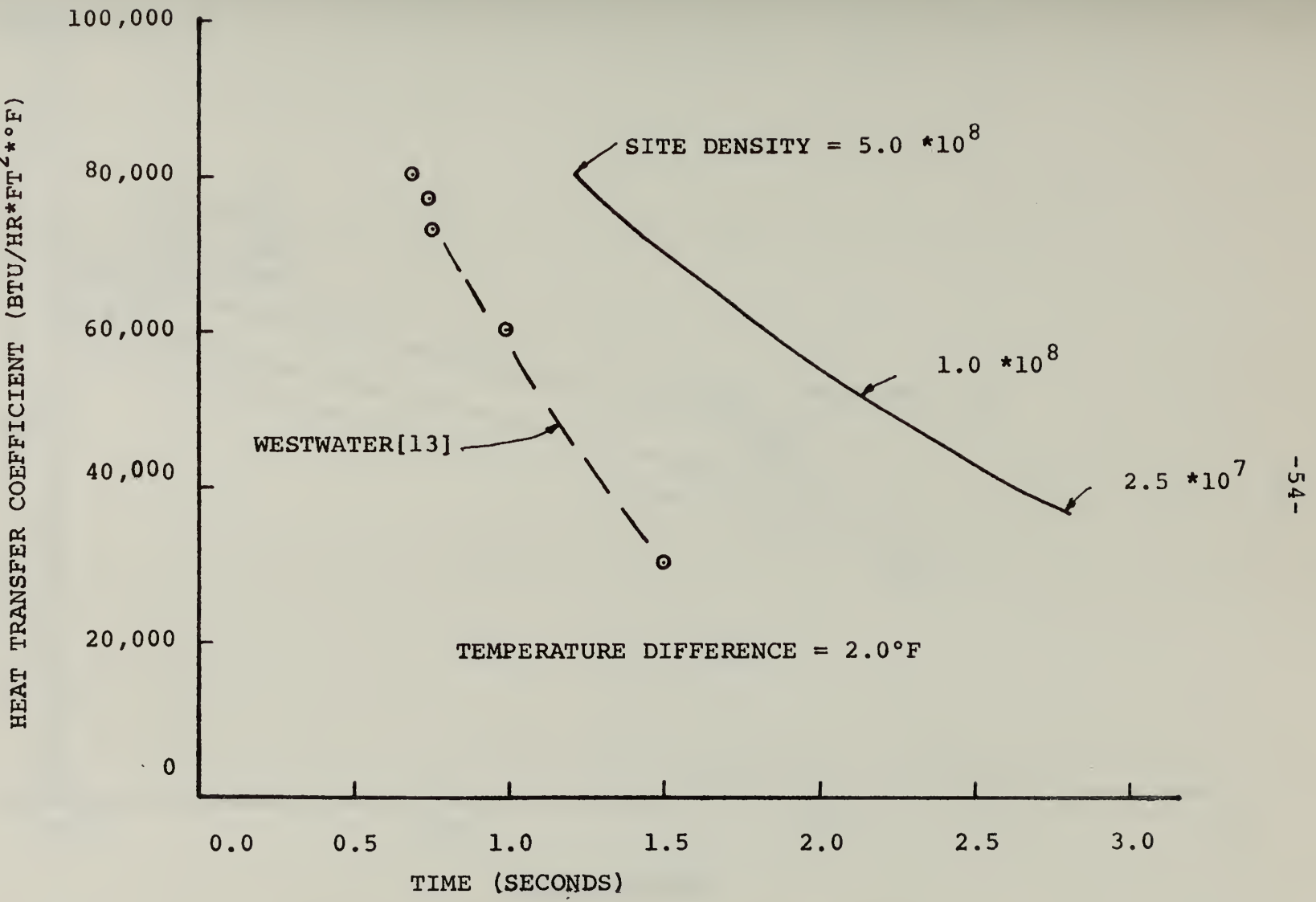

FIGURE 17 COMPARISON OF PREDICTED AND MEASURED TIME NECESSARY TO PRODUCE A DROP OF THE DEPARTING SIZE

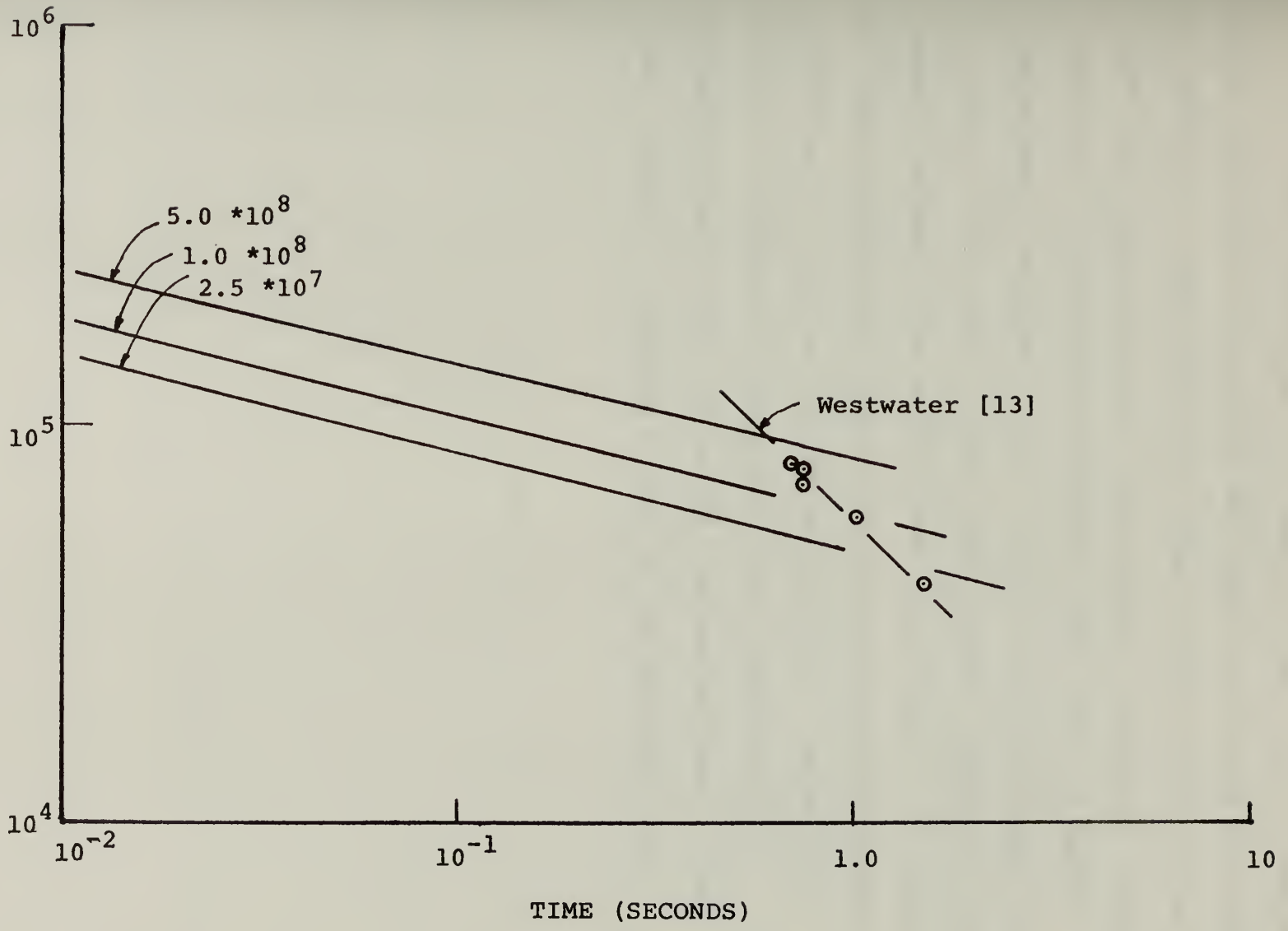

FIGURE 18 TIME COMPARISON OF TIME AVERAGED HEAT TRANSFER COEFFICIENTS WITH MEASURED COEFFICIENTS

The simulation is a model of the start of condensing on an initially bare surface and does not include the effect of sweeping. Experimentally, drops of the departing size slide down the surface and sweep vertical strips of the surface bare. In these bare regions, drops grow and appear approximately uniform in size. Since a drop can depart at any time in the actual steady state process, adjacent strips contain uniform drops of different generations. The regions of drops of different generations interact and may hasten the production of drops of the departing size. The model's failure to account for sweeping or the hemispherical assumption may be the reason for the overestimate of the time necessary to produce a drop of the departing size.

CHAPTER IV

CONCLUSIONS

1. Graham's model of heat flux through a single drop is a valid representation of the physical phenomenon.

2. As the site density increases, the heat transfer coefficient increases because of a greater number of small drops in the distribution.

3. For a temperature difference greater than one degree, the measured heat transfer coefficient remains constant because the site density is constant. For temperature differences less than one degree, the decrease in measured coefficients can be explained by a reduction in the site density.

4. As the saturation temperature decreases from 212°F to 88°F, the active nucleation site density decreases.

5. The model predicts a time necessary to produce a drop of the departing size which is twice as large as is observed for the steady state process.

6. This computer simulation provides a method of accurately predicting the heat transfer properties of the dropwise condensation process.

CHAPTER V

SUGGESTIONS FOR FUTURE WORK

1. The present model can be improved by using finer time steps and more elaborate starting technique for the later stages. Incorporation of the sweeping effect should also be added so that the simulation will more closely model the steady state process.

2. The effect of non-hemispherical drops may require investigation. A combination of experimental observations and a theoretical analysis should determine the effect, if any, of non-hemispherical drops.

REFERENCES

1. Rohsenow, W. M. and Choi, H., Heat, Mass, and Momentum Transfer, Prentice-Hall, Inc., Edgewood Cliffs, New Jersey (1961).

2. Graham, C., "The Limiting Heat Transfer Mechanism of Dropwise Condensation," Ph.D. Thesis, M.I.T. (1969).

3. Schmidt, E., Schurig, W., and Sellschopp, W., "Versuche iider die Kondensation von Wasserdampf in Film-und Tropfenform," Tech. Mech. Thermo-Dynam., 1, p. 53 (1930).

4. Jacob, M., "Heat Transfer in Evaporation and Condensation II," Mechanical Engineers, 58, p. 729 (1936).

5. Eucken, A., Naturwiss, 25, p. 209 (1937).

6. Emmons, H., "The Mechanism of Drop Condensation," Transactions A.I.Ch.E., 35, p. 109 (1939).

7. Tammann, Von. G., and Boehme, W., "Die Zuhl der Wassertropfchen he der Kondensation auf verschiedenen festen Stoffen," Annelen der Physik, 5, p. 22 (1935).

8. Umur, A. and Griffith, P., "Mechanism of Dropwise Condensation," ASME, Paper No. 64-WA/HT-3 (1964).

9. Le Fevre, E. J. and Rose, J. W., "A Theory of Heat Transfer by Dropwise Condensation," Proc. Third Int. Heat Trans. Conference, 2, p. 362 (1966).

10. Rose, J. W., "On the Mechanism of Dropwise Condensation," Int. J. Heat Mass Transfer, 10, p. 755 (1967).

11. Gose, E. E., Mucciardi, A. N. and Baer, E., "Model for Dropwise Condensation on Randomly Distributed Sites," Int. J. Heat Mass Transfer, 10, p. 15 (1967).

12. Tanasawa, I. and Tachibana, F., "A Synthesis of the Total Process of Dropwise Condensation Using the Method of Computer Simulation," University of Tokyo, Tokyo, Japan (1969).

13. Tower, R. E. and Westwater, J. W., "Effect of Plate Inclination on Heat Transfer During Dropwise Condensation of Steam," Chemical Engineering Symposium Series, 66, p. 21 (1970).

14. Nabavian, K. and Bromley, L. A., "Condensation Coefficient of Water," Chem. Eng. Sci., 18, p. 651 (1963).

15. Mikic, B. B., "On Mechanism of Dropwise Condensation," Int. J. Heat Mass Transfer, 12, p. 1311 (1969).

APPENDIX A

MODEL OF DROP GROWTH DUE TO CONDENSATION

Graham [2] proposed an analytical model for the growth of a single drop due to condensation of vapor. The heat flux associated with the condensing of vapor passes through three independent series resistances. The heat transfer resistances included are curvature, interfacial, and conduction. Each of these resistances is discussed below.

1. Curvature Resistance. At a curved liquid-vapor interface, the saturation temperature of the vapor in equilibrium with the drop is less than the saturation temperature of the vapor in equilibrium with liquid at a flat interface at the same pressure. A derivation of the temperature drop through the interface due to curvature can be found in Graham's thesis. The result of his work is reproduced below:

$$\Delta T_c = \frac{2T_s\sigma}{H_{fg}\rho} \frac{1}{r} \qquad \text{(A.1)}$$

where ΔT_c temperature drop due to curvature

T_s saturation temperature

σ surface tension

H_{fg} latent heat of transformation

ρ liquid density

r drop radius

When the total temperature difference available between the vapor and the condensing surface is equal to the temperature drop due to curvature, the minimum drop size which can exist on the surface is determined. The expression for minimum drop radius is written below:

$$r_{min} = \frac{2T_s\sigma}{H_{fg}\rho} \quad \frac{1}{\Delta T_t} \tag{A.2}$$

where ΔT_t the total temperature difference between the vapor and the condensing surface.

By combining the two previous equations, an expression for the temperature difference due to curvature can be found.

$$\Delta T_c = \frac{r_{min}}{r} \Delta T_t \tag{A.3}$$

where ΔT_c the temperature difference due to curvature.

This temperature difference is not an actual resistance to heat transfer, but can be thought of as an equivalent resistance.

2. Interfacial Mass Transfer Resistance. At the liquid-vapor interface, a pressure difference is necessary to force the mass transfer. The pressure difference can be converted into a temperature difference and is written below:

$$\Delta T_i = \frac{Q}{h_i 2\pi r^2} \tag{A.4}$$

Where Q rate of heat transfer

h_i interfacial heat transfer coefficient

ΔT_i temperature drop due interfacial resistance.

The interfacial coefficient, h_i, can be calculated from the equation below which was derived by Nabavian and Bromley [14].

$$h_i = \left(\frac{2\alpha}{2-\alpha}\right) \left(\frac{M}{2\pi \bar{R} T_s}\right)^{1/2} \frac{H_{fg}^2}{T_s V_g} \qquad (A.5)$$

where α condensation coefficient (assumed to be unity).

M molecular weight

$\bar{R}$ universal gas constant

V_g specific volume of the vapor.

Figure A-1 is a plot of the interfacial heat transfer coefficient as a function of saturation temperature.

3. Conduction Resistance. The most significant resistance associated with the liquid drop is the resistance to heat conduction through the drop. The conduction resistance of

$$R_{cyl} = \frac{\Delta T}{Q} = \frac{r}{K\pi r^2} \qquad (A.6)$$

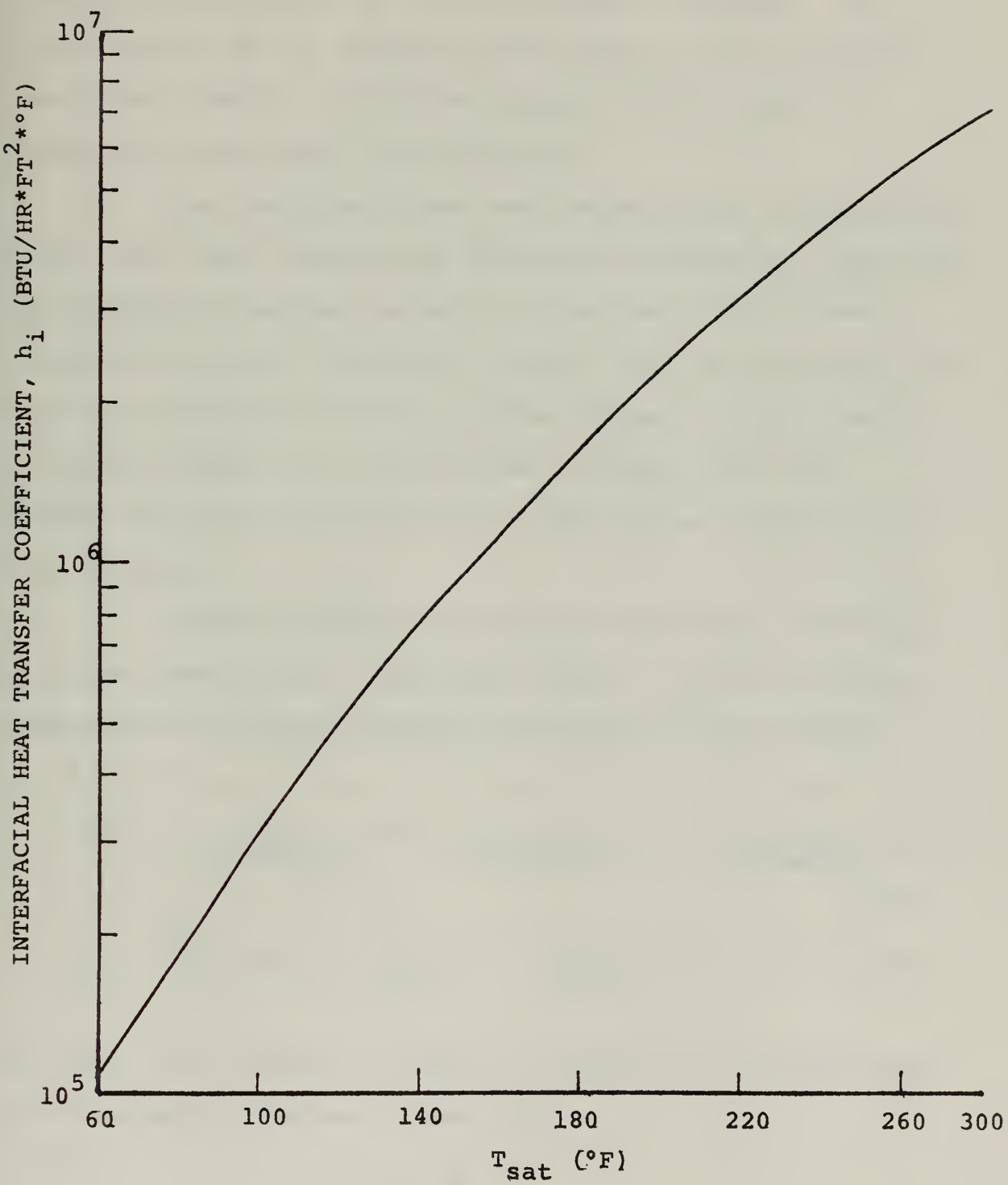

FIGURE A-1 VARIATION OF INTERFACIAL HEAT TRANSFER COEFFICIENT WITH TEMPERATURE. REPRODUCED FROM GRAHAM [2].

this shift. The age discrepancy is initially about 4×10^{-5} seconds and decreases as the drop radius increases. The error induced by the imprecise knowledge of the nucleation size should not be significant because little vapor is condensed in the small time interval.

Each resistance has been expressed as a temperature drop. The total temperature difference between the vapor and the condensing surface is equal to the sum of the three resistance induced temperature drops. Then by utilizing the idea that the rate of heat transfer through a single drop is proportional to the drop volume increase with time, Graham obtained an expression for drop age as a function of drop diameter.

Graham's derivation is reproduced below starting with the summation of temperature drops. ΔT_t is the total temperature difference between the vapor and the surface.

$$\Delta T_t = \underset{\text{(curvature)}}{\Delta T_c} + \underset{\text{(interfacial)}}{\Delta T_i} + \underset{\text{(conduction)}}{\Delta T_{dc}} \qquad \text{(A.8)}$$

$$\Delta T_t = \frac{r_{min}}{r} \Delta T_t + \frac{Q}{h_i 2\pi r} + \frac{Qr}{4K\pi r^2} \qquad \text{(A.9)}$$

The heat flux through the drop is assumed to be proportional to the change in volume of the drop.

$$Q = \rho H_{fg} \frac{dV}{dt}$$

where Q rate of heat transfer

ΔT temperature across the cylinder

R_{cyl} conduction resistance of the cylinder

K thermal conductivity of liquid

r drop radius

For hemispherical drops, the above expression is multiplied by a shape factor of less than one. Mikic [15] determined the value of the shape factor to be one fourth.

Multiplying by the shape factor and then solving for the temperature drop through the hemispherical drop, an expression for conduction resistance is obtained:

$$\Delta T_{dc} = \frac{Qr}{4K\pi r^2} \qquad (A.7)$$

where ΔT_{dc} temperature drop through the drop due to conduction resistance.

Figures A-2 and A-3 are reproduced from Graham's thesis and indicated the effect of the three resistances on drop diameter as a function of drop age.

Graham [2], stated that nucleation radius was probably between one and two times the minimum drop radius. A drop of the minimum size has a theoretical zero growth rate. Several nucleation radii were examined to determine their effect. The curve of drop radius as a function of drop age kept essentially the same shape, but was shifted to the right as nucleation radius decreased. Figure A-4 illustrates

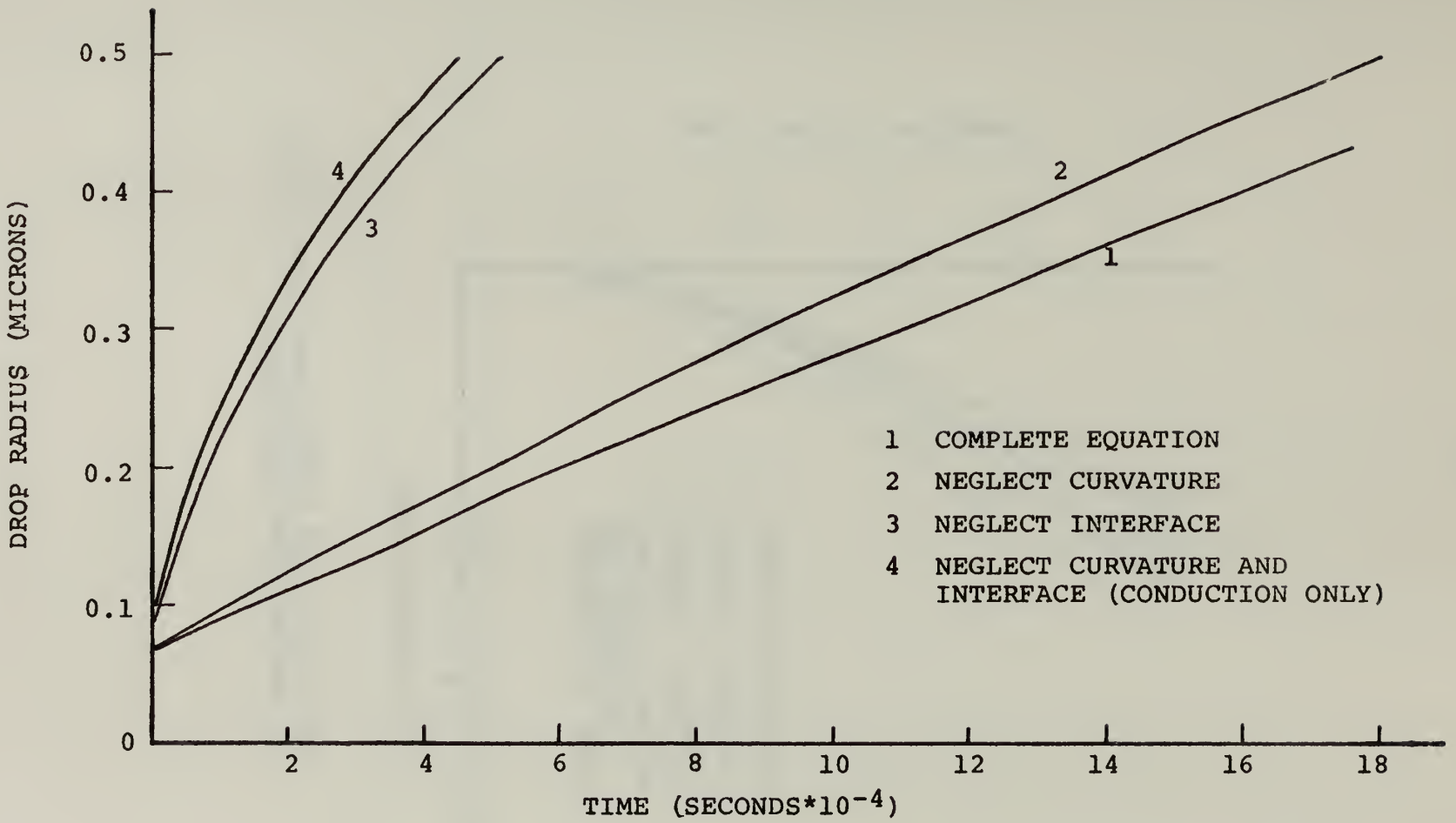

FIGURE A-2 DROP GROWTH RATE FOR 88°F.
REPRODUCED FROM GRAHAM [2].

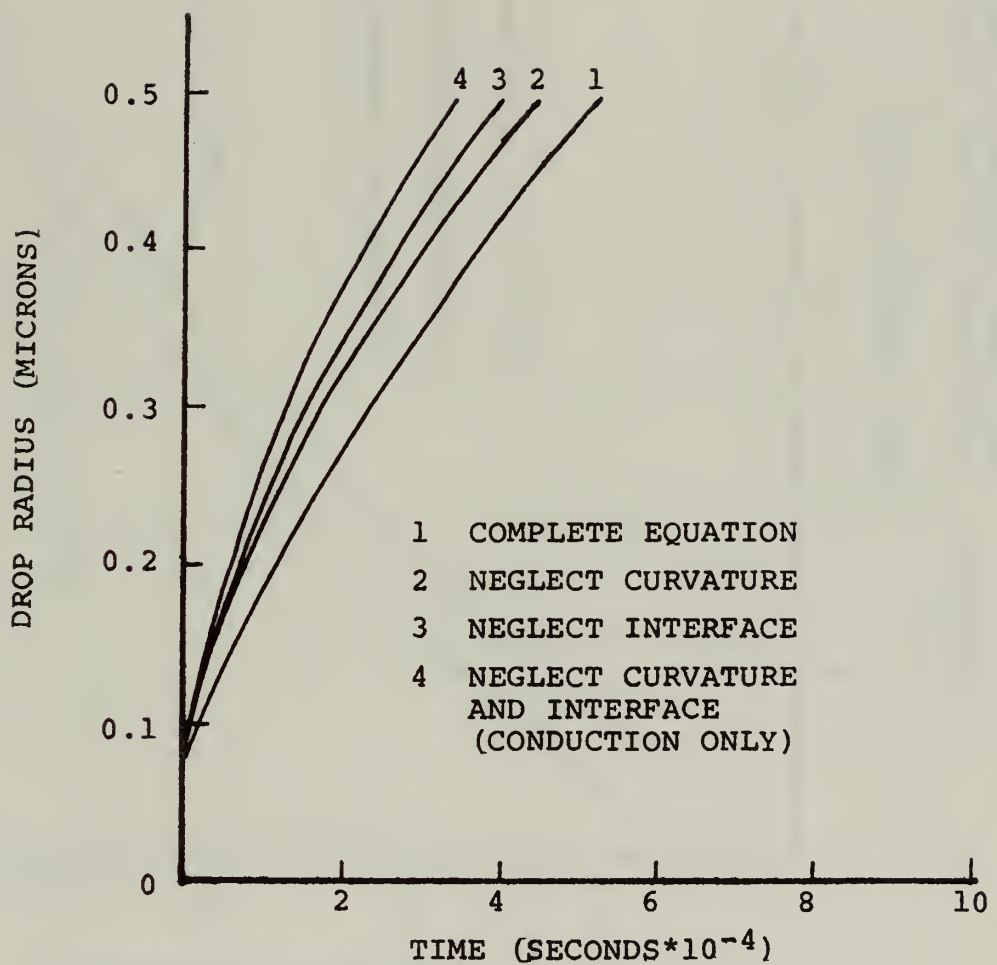

FIGURE A-3 DROP GROWTH RATE FOR 212°F.
REPRODUCED FROM GRAHAM [2].

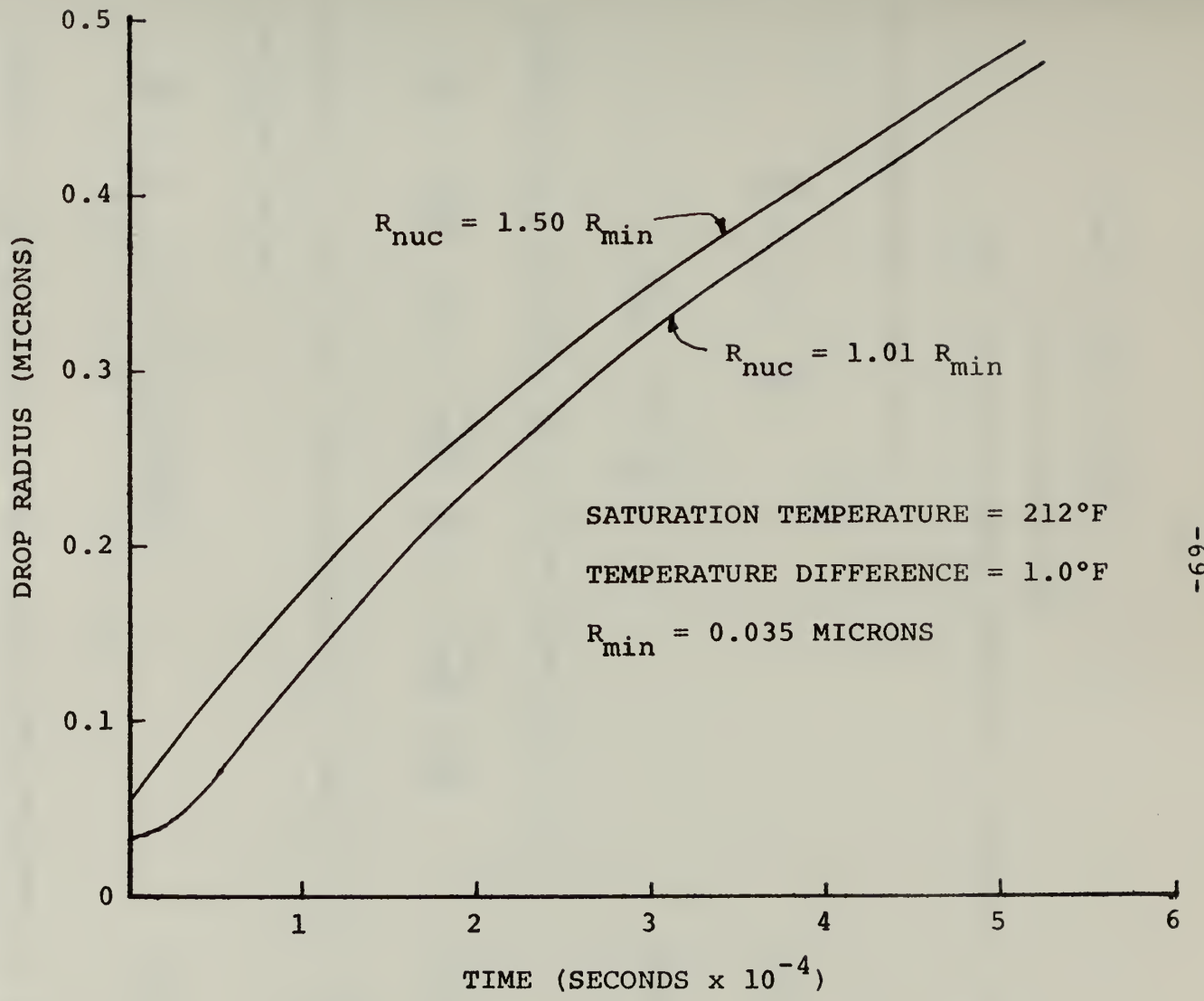

FIGURE A-4 VARIATIONS OF DROP GROWTH RATE WITH DROP NUCLEATION RADIUS

where V drop volume

t time or drop age

dV/dt change in drop volume with respect to time

For an hemispherical drop,

$$\frac{dV}{dt} = 2\pi r^2 \frac{dr}{dt} \tag{A.10}$$

$$Q = \rho H_{fg} \, 2\pi r^2 \frac{dr}{dt} \tag{A.11}$$

Substituting equation (A.11) into equation (A.9),

$$\Delta T_t = \frac{r_{min}}{r} \Delta T_t + \frac{\rho H_{fg}}{h_i} \frac{dr}{dt} + \frac{\rho H_{fg}}{2K} \frac{rdr}{dt} \tag{A.12}$$

Solving for dr/dt and substituting drop diameter D for twice the drop radius,

$$\frac{dD}{dt} = \frac{4}{\rho H_{fg}} \Delta T_t \left[\frac{1 - D_{min}/D}{D/2K + 2/h_i} \right] \tag{A.13}$$

Equation (A.13) can be integrated and then evaluated at the lower limit. Since the logarithmic terms become undefined at drop age zero when the drop diameter equals the minimum diameter, the function must be evaluated at the minimum diameter plus epsilon. Graham's final result of drop age as a function of drop diameter is listed below.

$$\frac{1}{2K}\left[\cdot\ S(D-D_{min})^2 + 2D_{min}(D-D_{min}) + D_{min}^2\ \ln\ (D-D_{min})\right]$$

$$+\ \frac{2}{h_i}\left[(D-D_{min}) + D_{min}\ \ln\ (D-D_{min})\right]$$

$$-\ \frac{1}{2K}\ D_{min}^2 - \frac{2}{h_i}\ D_{min} = \frac{4}{\rho H_{fg}}\ \Delta T_t t \qquad \text{(A.14)}$$

The simulation growth routine required an expression of drop radius as a function of age. For all cases in this study, Graham's equation (A.14) was inverted by substituting a constant equal to five minimum drop diameter for the diameter variable in the logarithmic terms. This action converts the logarithmic expressions into constants. The inverstion is then finished by completing the square. The final result (A.15) is an analytical approximation for drop diameter as a function of drop age and is shown below:

$$D = \sqrt{\frac{d}{a}\ t - \frac{c}{a} + \frac{b}{4a^2}} - \frac{b}{2a} \qquad \text{(A.15)}$$

where $a = 1/4K$

$b = D_{min}/2K + 2/h_i$

$c = 5\ D_{min}^2/4K - 4D_{min}/h_i$

$\quad + (D_{min}^2/2K + 2D_{min}/h_i)\ \ln\ (4D_{min})$

$d = 4\Delta T_t/\rho H_{fg}$

The approximation has reasonable accuracy over almost all of the range of drop sizes. The greatest inaccuracy experienced for the condensing conditions of this study was about two percent for drop radii of less than one micron. As the drop radius increased above one micron, the inaccuracy rapidly diminished.

Using equations (A.14) and (A.15), the drop growth routine can be carried out. First a drop's age is determined using equation (A.14). The age calculated is then increased by the time step. Finally, the new size of a drop is calculated with expression (A.15).

APPENDIX B

COALESCENCE ROUTINE

The coalescence routine developed is capable of determining coalescence of drops, blanketing of drop sites or locations, and the uncovering of sites. Four variables associated with each site are required for the routine to operate with either randomly or uniformly distributed sites. The first two of the four site variables are coordinates, "X" and "Y". These are obtained by superimposing a first quadrant coordinate system on the stage area. The coordinates of sites are necessary to calculate the distances between sites. Then the sites are ordered from left to right on the stage square and assigned index numbers represented by the variable "I". The site with the lowest X coordinate value is site number one; the site with the highest X coordinate value has the largest index number. The fourth variable, "R", identifies the activity at the site. The "R" variable can assume three types of possible values; minus one, zero, or a finite positive number. The minus one value indicates that the site is covered or blanketed by a drop centered on another site. The zero value represents a site that is exposed to the vapor or uncovered. The third "R" value is a finite positive number which is the radius of a drop in feet centered on the site. Touching of drops and covering of nucleation sites is determined by comparison of

the distance between sites and the drop radius. These four site variables; "X, Y, I, and R"; are necessary to perform the bookkeeping required by the coalescence activity.

The coalescence routine commences for each time step at the site with the lowest index number with a drop centered on it and proceeds until the site with a drop and the highest index number is examined for possible coalescences. A search area around the "Ith" drop of interest is defined as a square of two "Ith" drop diameters on a side. Figure B-1 is a diagram of a search square on the simulated condensing surface. Sites with a zero "R" value or a positive "R" value inside the square are examined. A determination is made whether or not the "Ith" drop with its increased radius from condensation growth blankets any uncovered or active sites. At the same time, a check for the possible coalescence between the central "Ith" drop and a neighboring "Jth" drop with a center inside the square is conducted. Only neighboring drops of the same size or smaller are not examined even though they may be blanketing part of the search or even touching the central drop.

By maintaining a consistant examining procedure as the routine moves from drop to drop and from left to right on the simulated surface, all possible coalescences are found. This approach requires a relatively small amount of computer core storage and is reasonably efficient for one thousand

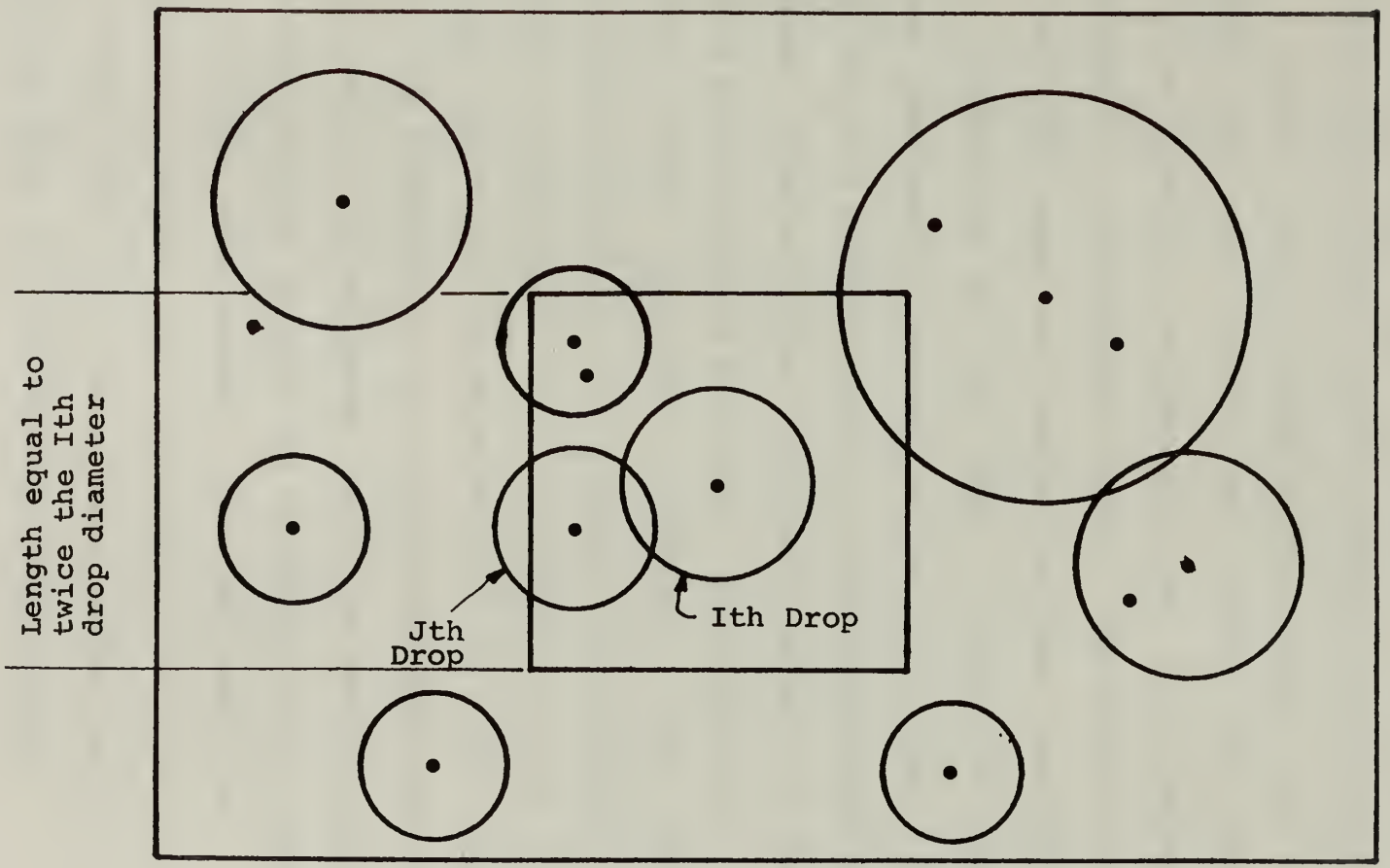

FIGURE B-1 SECTION OF STAGE AREA WITH SEARCH SQUARE CENTERED ON ITH DROP

sites on a stage area. For large numbers of small drops, small search areas are used. For the small number of large drops, large search areas are employed. This flexibility is the principle reason for the routine's efficiency.

When a site is found to be covered, its "R" value is changed from zero to minus one. If the "Ith" drop is found to be touching a neighboring "Jth" drop inside the search square, a coalescence occurs. The masses of the "Jth" and "Ith" drops are combined to form a new drop at the central location of the "Ith" drop. A check for uncovering of sites, previously blanketed by the "Jth" drop, is then carried out in a similar manner as the coalescence was determined. When all sites previously covered by the "Jth" drop have been found and uncovered, the search for coalescence starts once again by defining a new larger search square around the "Ith" drop. The increased size of the square is indicative the the increase in size of the "Ith" drop due to the coalescence with the "Jth" drop. When no more coalescences are obtained between the "Ith" drop and any of its neighbors inside the search square, the coalescence routine centers its attention on the drop of the next higher index number. The same search for coalescence, covering, and uncovering is carried out. When the drop with the highest index number fails to touch a neighboring drop, the coalescence routine ends.

APPENDIX C

DESCRIPTION OF THE INPUT DATA

Seven data cards are used to read in fifteen variables necessary to run the program. These variables will be discussed in the order which they are read in.

1. First Data Card

Variable Name: IX

Format: I9

Description: The variable "IX" is any number with nine or less integers so long as the last integer is odd. The number is necessary to call a random number generator which is the IBM Scientific Subroutine RANDU. The random number generator is used to create the random site location for the first stage. If fewer than one hundred sites are used for the first stage, the selection of the variable "IX" can cause the time averaged heat transfer coefficient at the end of the first stage to vary by as much as ten percent.

2. Second Data Card

Variable Names: NN, SCALE

Format: I10, F10.4

Description: These two variables determine the site density. "NN" is the number of sites for the first stage. "SCALE" is the dimension of the side of the first stage square. Scale is read in units of microns and then converted into feet in the program. (The program does most of its

calculations in English Engineering Units.) Any number of "NN" sites can be used, but the scale can be only 10.0, 31.623, 100.0, 316.23, or 1000.0 microns. Site densities up to ten to the ninth sites per square centimeter can be accommodated. (The program ran more efficiently by not letting the number of sites exceed one thousand on the initial stage area.)

3. Third Data Card

Variable Names: MM, TSTEP

Format: I10, E11.4

Description: "MM" is the number of time steps allowed for each stage. A limit of one thousand should not be exceeded. "TSTEP" is the time step for the first stage. The value selected should be large enough so that drops originating from nucleation sites have a radius which is three or more times larger than the minimum drop radius. The growth models inaccuracy for very small drops dictates this constraint. TSTEP has the units of seconds.

4. Fourth Data Card

Variable Names: TSAT, SURTE, HEATL, THCON, DTEMT, FDEN, HTCI

Format: 6F10.4, E11.4

Description:

"TSAT" is the saturation temperature of the vapor for a flat vapor-liquid interface in degrees Rankine.

"SURTE" is the surface tension of the liquid at the saturation temperature and has the units of pounds force per foot.

"HEATL" is the latent heat of transformation of the vapor to the liquid at the saturation temperature. Its units are British Thermal Units per pound mass.

"THCON" is the thermal conductivity of the liquid at the saturation temperature and has the units of British Thermal Units per foot-hour-degree absolute.

"DTEMT" is the temperature difference between the vapor and the base of the drop which is approximated by the average surface temperature. The units are degrees Rankine.

"FDEN" is the liquid's density in pounds mass per cubic foot.

"HTCI" is the interfacial heat transfer coefficient and was obtained from a graph of values for various saturation temperature in Graham's thesis [2]. The coefficient has the units of British Thermal Units per square foot-hour-degree absolute.

5. Fifth Data Card

Variable Name: RNUC

Format: F6.3

Description: "RNUC" is the size chosen for the nucleating drops necessary for the math model of condensation

growth. Graham [2] stated that the nucleation size was probably between one and two times the minimum diameter. This simulation used a nucleation drop radius of one and a half times the minimum radius. The "RNUC" value for this case is the factor one point five.

6. Sixth Data Card

Variable Name: RMAX

Format: F10.4

Description: "RMAX" is the radius in microns of a drop of the departing size.

The values used in this study were determined by Graham [2]. For a temperature difference of one-half degree, Graham measured values of 1500 microns and 1250 microns for the saturation temperatures of 88 and 212 degrees Fahrenheit respectively. Values of 1125 and 1375 microns were assumed for the saturation temperatures of 274 degrees and 150 degrees. (For this study, the maximum drop size was assumed to remain constant for all temperature differences.)

APPENDIX D

PROGRAM SOURCE LISTING

The computer simulation of this study consists of a single program written in Fortran IV, Level G, for use on the IBM Model 360/65 Digital Computer. The following pages of this appendix contain a source listing of the program.

```
C      SOURCE LISTING FOR COMPUTER SIMULATION OF THE DROPWISE
      1CONDENSATION PROCESS
C      SPRING, 1971
C      THE PROGRAM IS WRITTEN FORTRAN IV, LEVEL G
C      THE COMPUTER USED FOR THE STUDY WAS THE IBM MODEL 360/65
       DIMENSION X(2000), Y(2000), R(2000), RM(2000)
       DIMENSION NUMB(15), TT(15), SS(15)
       DIMENSION WTT(35), WSS(35), AWSS(35), BWSS(35), DELN(35)
       DIMENSION FACTOR(10), BBAREA(10), TTIME(10), AAREA(10), PA(35)
       DIMENSION KKV(10), KVV(10)
       DIMENSION WSSF(35), HTCD(35)
       DIMENSION HTC(1000), THTC(1000)
       DIMENSION TIME1(1000), BAREA1(1000)
       DIMENSION NWSS(35)
       READ(5,100) IX
  100  FORMAT(I9)
       READ(5,101)  NN, SCALE
  101  FORMAT(I10,F10.4)
       READ(5,102) MM, TSTEP
  102  FORMAT(I10,E11.4)
       READ(5,103) TSAT, SURTE, HEATL, THCON, DTEMT, FDEN, HTCI
  103  FORMAT(6F10.4,E11.4)
       READ(5,104) RNUC
  104  FORMAT(F6.3)
       READ(5,106) RMAX
  106  FORMAT(F10.4)
       READ(5,107) RSTD
  107  FORMAT(F10.4)
       WRITE(6,200) IX
  200  FORMAT(1X,'IX=',I9)
       WRITE(6,201) NN, SCALE
  201  FORMAT(1X,'NN=',I10,' SITES',5X,'SCALE=',F10.4,' MICRONS')
       WRITE(6,202) MM, TSTEP
  202  FORMAT(1X,'MM=',I10,' TIME STEPS',5X,'TSTEP=',E11.4,' SECONDS')
       WRITE(6,203) TSAT, SURTE, HEATL
  203  FORMAT(1X,'TSAT=',F10.4,' DEGREES ABS.',5X,'SURTE=',F10.4,' LBF. P
```

```
     1ER FT.',5X,'HEATL=',F10.4,' BTUS PER LBM.')
      WRITE(6,204) DTEMT, HTCI, THCON
  204 FORMAT(1X,'DTEMT=',F10.4,' DEGREES ABS.',5X,'HTCI=',E11.4,' BTUS P
     1ER FT.**2 HR. DEG. ABS.',5X,'THCON=',F10.4,' BTUS PER FT. HR. DEG.
     1 ABS.')
      WRITE(6,205) FDEN, RNUC
  205 FORMAT(1X,'FDEN=',F10.4,' LBM. PER FT.**3',5X,'RNUC=',F8.4,' *MINI
     1MUN RADIUS')
      SCALE=SCALE*3.2808E-6
      AREA=SCALE*SCALE
      SDEN=NN/(AREA*144.0*2.54*2.54)
      WRITE(6,206) SDEN
  206 FORMAT(1X,'SDEN=',E11.4,' SITES PER CM**2')
      WRITE(6,220) RMAX
  220 FORMAT(1X,'RMAX=',F10.4,' MAXIMUN RADIUS IN MICRONS')
      WRITE(6,207) RSTD
  207 FORMAT(1X,'RSTD=',F10.4,'  ZERO MODEL ERROR AT RADIUS .EQ. RSTD')
      RMIN=(2.0*TSAT*SURTE*1.285E-3)/(HEATL*FDEN*DTEMT)
      RMINM=RMIN/3.2808E-6
      RNUC=RNUC*RMIN
      RSTD=RSTD*RMIN
      CA=1.0/THCON
      CB=(2.0*RMIN)/THCON +4.0/HTCI
      CC=(2.0*RMIN**2)/THCON +(2.0*RMIN)/HTCI
      DA=CA*RNUC**2
      DB=CB*RNUC
      DC=CC*ALOG(2.0*RNUC-2.0*RMIN)
      CX=(FDEN*HEATL*3600.)/(4.0*DTEMT)
      CD=DA+DB+DC
C     AGE=CX( CA*RADI**2 + CB*RADI + CC*ALOG(2.0*RADI-2.0*RMIN) - CD)
C     AGE IS A FUNCTION OF DROP RADIUS
      FA=CX*CA
      FB=CX*CB
      FC=CX*CC
      FD=CX*CD
C     AGE=FA*RADI**2 + FB*RADI + FC*ALOG(2.0*RADI-2.0*RMIN) - FD
```

```
C      NOW START COMPUTATION OF RADIUS AS A FUNCTION OF AGE
       CE=CC*ALOG(2.0*RSTD-2.0*RNUC)-CD
       FA=1.0/(CX*CA)
       EB=CB**2/(4.0*CA**2) - CE/CA
       EC=CB/(2.0*CA)
C      CRADI=SQRT(AGE*EA+EB) -EC
       WRITE(6,210) RMIN, RMINM
  210  FORMAT(1X,'RMIN=',E11.4,' FEET',5X,'RMINM=',F8.4,' MICRONS')
       WRITE(6,212) FA, FB, FC, FD
  212  FORMAT(1X,'FA=',E11.4,3X,'FB=',E11.4,3X,'FC=',E11.4,3X,'FD=',
      1E11.4)
       WRITE(6,213) EA, EB, EC
  213  FORMAT(1X,'EA=',E11.4,3X,'EB=',E11.4,3X,'EC=',E11.4)
       VOLDO=(2.0*3.1416*RNUC*RNUC*RNUC)/3.0
C
C      CALCULATION OF DISTRIBUTION
       ARW=RMAX
       WTT(35)=ARW
       DO 599 I=1,35
       ARV=ARW/1.20
       WSS(36-I)=ARV
       ART=ARV*0.80
       IF(I .EQ. 35) GO TO 609
       WTT(35-I)=ART
       ARW=ART
  599  CONTINUE
  609  CONTINUE
       WRITE(6,575) (WSS(I), I=1,35)
  575  FORMAT(10F12.5)
       WRITE(6,576) (WTT(I), I=1,35)
  576  FORMAT(10F12.5)
C      END OF CLACULATION OF DISTRIBUTION
C
       DO 603 I=1,10
       TTIME(I)=0.0
       AAREA(I)=0.0
```

```
      KKV(I)=0.0
      KVV(I)=0.0
  603 CONTINUE
C     INITIALIZING THE NWSS ARRAY
      DO 582  I=1,35
      NWSS(I)=0
      AWSS(I)=0.0
      BWSS(I)=0.0
  582 CONTINUE
      MSTAGE=1
   71 CONTINUE
      ISS2=1
      NSS2=1
      KIR=1
      STD=0.01
      STDU=STD
      STDL=-STD
C
C     COMMENCE SELECTION OF DISTRIBUTION AND TERMINATION CRITERIA
      AGOR=SCALE/3.2808E-06
      IF(AGOR .LT. 3.20) GO TO 641
      IF(AGOR .LT. 11.0) GO TO 561
      IF(AGOR .LT. 32.0) GO TO 562
      IF(AGOR .LT. 110.0) GO TO 563
      IF(AGOR .LT. 320.0) GO TO 564
      IF(AGOR .LT. 1100.0) GO TO 565
      IF(AGOR .LT. 3200.0) GO TO 566
      IF(AGOR .LT. 11000.0) GO TO 567
      IF(AGOR .LT. 19000.0) GO TO 567
      WRITE(6,572)
  572 FORMAT(6X,'SCALES DID NOT MATCH')
      GO TO 89
  641 CONTINUE
      ULIMIT=0.56
      GO TO 569
  561 CONTINUE
```

```
      ULIMIT=1.78
      GO TO 569
  562 CONTINUE
      ULIMIT=5.67
      GO TO 569
  563 CONTINUE
      ULIMIT=17.8
      GO TO 569
  564 CONTINUE
      ULIMIT=56.7
      GO TO 569
  565 CONTINUE
      ULIMIT=178.
      GO TO 569
  566 CONTINUE
      ULIMIT=567.0
      GO TO 569
  567 CONTINUE
      ULIMIT=RMAX
      GO TO 569
  569 CONTINUE
C
C     INITIALIZING DISTRIBUTION LIMITS AND HEADINGS
      DO 573 I=1,15
      TT(I)=0.0
      SS(I)=0.0
  573 CONTINUE
C
C     DO 577 LOOP, DETERMINATION OF KV VALUE
C     KV VALUE DETERMINED THE TERMINATION CRITERIA
      DO 577 I=1,35
      RUV=ULIMIT-WTT(I)
      IF(RUV) 579, 578, 577
  577 CONTINUE
  578 KV=I
      GO TO 580
```

```
  579  KV=I-1
  580  CONTINUE
       WRITE(6,606) KV
  606  FORMAT(6X,'KV=',I10)
       IR=MSTAGE
       KKV(IR)=KV
       KVV(IR)=KKV(IR)-12
       AF=WSS(KV)*WSS(KV)*3.1416*3.2808E-06*3.2808E-06
C
C      DO 581 LOOP SETS THE LIMITS AND HEADINGS FOR THE STAGE DROP
      1DISTRIBUTIONS
       LOR=KV+1
       DO 581 I=1,15
       TT(16-I)=WTT(LOR-I)
       SS(16-I)=WSS(LOR-I)
  581  CONTINUE
       WRITE(6,618) (SS(I), TT(I), I=1,15)
  618  FORMAT(F10.4,6X,F10.4)
       IF(MSTAGE .EQ. 1) GO TO 570
C
C      COMMENCE STAGE START UP ITERATION
C      ITERATION VARIABLES ARE NR1 AND HCK
       LC=1
       HEAT1=(THTC1*TSTEP*AREA*DTEMT)/3600.
       TVOL1=HEAT1/(FDEN*HEATL)
       ARR1=(3.0*TVOL1)/(2.0*3.1416)
   94  RMF1=(ARR1/NR1)**.3333333
       RMM1=RMF1/3.2808E-06
       VPD1=(RMF1*RMF1*RMF1*3.1416*2.0)/3.0
       AGE=FA*RMF1*RMF1 +FB*RMF1 +FC*ALOG(2.0*RMF1-2.0*RMIN) -FD
       AGE=AGE+TSTEP
       RMF12=SQRT(AGE*EA+EB)-EC
       RMM12=(RMF12/3.2808E-06)
       VPD12=(2.0*3.1416*RMF12*RMF12*RMF12)/3.0
       VCG12=(VPD12-VPD1)*NR1
       DAREA=(3.1416*RMF1*RMF1)*NR1
```

```
      SAREA=AREA-DAREA
      HEATHH=(THTC1*DTEMT*SAREA*TSTEP)/3600.
      CHEAT2=HEATHH+(VCG12*FDEN*HEATL)
      THEAT2=(THTC2*2.0*TSTEP*AREA*DTEMT)/3600.
      EHEAT2=THEAT2-HEAT1
      HCK=(EHEAT2-CHEAT2)/EHEAT2
      IF(HCK .GT. STDL .AND. HCK .LT. STDU) GO TO 92
      WRITE(6,700) LC, NR1, RMM1, HCK, RMM12
  700 FORMAT(6X,'LC=',I8,6X,'NR1=',I8,6X,'RMM1=',F10.4,6X,'HCK=',F10.4,
     16X,'RMM12=',F10.4)
      NR1=NR1-5
      LC=LC+1
      IF(LC .EQ. 99) GO TO 746
      GO TO 94
C     CHANGE OF STANDARD FOR CONVERGENCE
  746 STD=STD*3.0
      KIR=KIR+1
      IF(KIR .EQ. 4) GO TO 89
      STDU=STD
      STDL=-STD
      LC=1
      NR1=500
      WRITE(6,709) STD
  709 FORMAT(6X,'STANDARD FOR CONVERGENCE=',F10.4)
      GO TO 94
   92 CONTINUE
      NR=NR1
      WRITE(6,701) LC, NR1, RMM1, HCK, RMM12
  701 FORMAT(6X,'LC=',I8,6X,'NR1=',I8,6X,'RMM1=',F10.4,6X,'HCK=',F10.4,
     16X,'RMM12=',F10.4)
C     END OF START UP ITERATION
C
C     MATCHING NN AND NR1+NR2
      NR2=NR1
      NNL1=NR1+NR2
      NNL=SCALE/(2.0*1.0001*RMF1)
```

```
      NNLT=NNL*NNL
      NN=NNLT
      WRITE(6,708) NR1, NNL1, NNL, NNLT
  708 FORMAT(6X,'NR1=',I10,6X,'NNL1=',I10,6X,'NNL=',I10,6X,'NNLT=',I10)
      RSTART=RMF1
      VSTART=(2.0*RSTART*RSTART*RSTART*3.141)/3.0
      VCHGS=VSTART-VOLDO
C     END OF MATCHING NR1 AND NN
C
C     UNIFORM DISTRIBUTION OF SITES NNL BY NNL
      ABC=(2.0*1.0001*RMF1)/SCALE
      KR=0
      DO 35 J=1,NNL
      DO 34 I=1,NNL
      KR=KR+1
      X(KR)=ABC*J
   34 CONTINUE
   35 CONTINUE
      KKR=0
      DO 36 J=1,NNL
      DO 70 I=1,NNL
      KKR=KKR+1
      Y(KKR)=ABC*I
   70 CONTINUE
   36 CONTINUE
C     END OF UNIFORM DISTRIBUTION OF SITES
      GO TO 571
  570 CONTINUE
C
C     GENERATION AND ORDERING OF RANDOM SITES
      DO 11 I=1,NN
      CALL RANDU(IX,IY,A)
      X(I)=A
      IX=IY
   11 CONTINUE
      KK=1
```

```
      NNS=NN-1
   15 DO 12 I=KK,NNS
      IF(X(I+1)-X(KK)) 13,12,12
   13 AA=X(KK)
      X(KK)=X(I+1)
      X(I+1)=AA
   12 CONTINUE
      KK=KK+1
      IF(KK .LE. NNS) GO TO 15
      DO 16 I=1,NN
      CALL RANDU(IX,IY,A)
      Y(I)=A
      IX=IY
   16 CONTINUE
C     END OF GENERATION OF SITES
  571 CONTINUE
C
C     MULTIPLY CO-ORDINATE BY SCALE
      DO 39 I=1,NN
      X(I)=X(I)*SCALE
      Y(I)=Y(I)*SCALE
   39 CONTINUE
C     INITIAL RADIUS ARRAY DISTRIBUTION
      DO 38 I=1,NN
      R(I)=0.000
   38 CONTINUE
C
C     COUNTER DO 3 LOOP
      TIME=0.0
      THEAT=0.00
      DO 3 II=1,MM
      TVCHG=0.000
C
C     FINITE DROPS GROW
      DO 4 I=1,NN
       IF(R(I)) 4,4,45
```

```
   45  AGE=FA*R(I)**2 + FB*R(I) + FC*ALOG(2.0*R(I)-2.0*RMIN) -FD
       VOLD=(2.0*3.1416*R(I)*R(I)*R(I))/3.0
       AGE=AGE+TSTEP
       R(I)=SQRT(AGE*EA+EB) -EC
       VNEW=(2.0*3.1416*R(I)*R(I)*R(I))/3.0
       VCHG=VNEW-VOLD
       TVCHG=TVCHG+VCHG
    4  CONTINUE
       IF(MSTAGE .EQ. 1) GO TO 553
C
C      RANDOM LOADER
       RMF=RMF1
   85  NC=1
   81  IF(NC .GT. NR) GO TO 83
   84  CALL RANDU(IX,IY,A)
       IX=IY
       NO=A*1000.
       IF(NO .EQ. 0) GO TO 84
       IF(NO .GT. NN) GO TO 84
       IF(R(NO)) 84,82,84
   82  R(NO)=RMF
       VCHG=VCHGS
       TVCHG=TVCHG+VCHG
       NC=NC+1
       GO TO 81
   83  CONTINUE
       GO TO 554
C      END OF RANDOM LOADER
C
C      ALL ZERO VALUE DROPS GROW FOR STAGE ONE
  553  CONTINUE
       DO 555 I=1,NN
       IF(R(I)) 555, 556, 555
  556  AGE=TSTEP
       R(I)=SQRT(AGE*EA+EB)-EC
       VNEW=(2.0*3.1416*R(I)*R(I)*R(I))/3.0
```

```
      VCHG=VNEW-VCLDC
      TVCHG=TVCHG+VCHG
  555 CONTINUE
C     END OF ZERO VALUE DROPS GROW
C
C     HEAT TRANSFER CALCULATIONS
  554 CONTINUE
      HEAT=FDEN*HEATL*TVCHG
      HTC(II)=(HEAT*3600.)/(TSTEP*AREA*DTEMT)
      THEAT=THEAT+HEAT
      TIME=TIME+TSTEP
      THTC(II)=(THEAT*3600.)/(TIME*AREA*DTEMT)
      WRITE(6,500) II, HTC(II)
  500 FORMAT(1X,I4,3X,'HTC=',E11.4)
      WRITE(6,402) TIME
  402 FORMAT(1X,'TIME=',E11.4)
      TIME1(II)=TIME
      WRITE(6,502) THTC(II)
  502 FORMAT(1X,'THTC=',E11.4)
C     END OF HEAT TRANSFER CALCULATION
C
C     COMMENCE COALESCENCE ROUTINE
      ICC=0
      N=1
      DO 1 I=1,NN
      IF(R(I) .LE. 0.0) GO TO 1
    8 S=X(I)-2.0*R(I)
   41 IF(X(N) .GT. S) GO TO 31
      N=N+1
      GO TO 41
   31 N=N-1
      IF(N .LE. 0) GO TO 7
      IF(X(N) .GT. S) GO TO 31
    7 N=N+1
      DO 2 J=N,NN
      IF(J .EQ. I) GO TO 2
```

```
      ST=X(I)+2.0*R(I)
      IF(X(J) .GT. ST) GO TO 1
      IF(R(J) .GT. R(I)) GO TO 2
      IF(R(J) .EQ. -1.0) GO TO 2
      SST=Y(I)+2.0*R(I)
      IF(Y(J) .GT. SST) GO TO 2
      SSTT=Y(I)-2.0*R(I)
      IF(Y(J) .LT. SSTT) GO TO 2
      SSS=R(I)+R(J)
      IF(ABS(X(I)-X(J)) .GT. SSS) GO TO 2
      IF(ABS(Y(I)-Y(J)) .GT. SSS) GO TO 2
      T=(X(I)-X(J))*(X(I)-X(J))+(Y(I)-Y(J))*(Y(I)-Y(J))
      TS=(R(I)+R(J))*(R(I)+R(J))
      IF(T .GT. TS) GO TO 2
C     A COALESCENCE HAS OCCURRED
      IF(R(J) .EQ. 0.0) GO TO 20
      R(I)=(R(I)*R(I)*R(I)+R(J)*R(J)*R(J))**.3333333
      ICC=ICC+1
      K=N
   96 SSSS=X(J)+R(J)
      IF(X(K) .GT. SSSS) GO TO 50
      IF(R(K) .GE. 0.0) GO TO 98
      IF(ABS(X(K)-X(J)) .GT. R(J)) GO TO 98
      IF(ABS(Y(K)-Y(J)) .GT. R(J)) GO TO 98
      TTV=((X(K)-X(J))*(X(K)-X(J)))+((Y(K)-Y(J))*(Y(K)-Y(J)))
      TTS=R(J)*R(J)
      IF(TTV .GT. TTS) GO TO 98
      R(K)=0.0
   98 K=K+1
      IF(K .GT. NN) GO TO 50
      GO TO 96
   20 R(J)=-1.0
      GO TO 2
   50 R(J)=0.0
      GO TO 8
    2 CONTINUE
```

```
    1  CONTINUE
       WRITE(6,305) ICC
  305  FORMAT(1X,'COALESCENCE COUNTER=',I10)
C      END OF COALESCENCE ROUTINE
C
C      COMMENCE DISTRIBUTION ANALYSIS
       RNUCM=RNUC/3.2808E-6
       DO 37 K=1,NN
       IF(R(K)) 46,47,48
   48  RM(K)=R(K)/3.2808E-6
       GO TO 37
   47  RM(K)=0.00
       GO TO 37
   46  RM(K)=-1.0
   37  CONTINUE
       DO 66 I=1,15
       NUMB(I)=0
   66  CONTINUE
       DO 67 I=1,NN
       IF(RM(I) .EQ. -1.00) GO TO 51
       IF(RM(I) .EQ. 0.00) GO TO 52
       IF(RM(I) .LT. TT(3)) GO TO 53
       IF(RM(I) .LT. TT(4)) GO TO 54
       IF(RM(I) .LT. TT(5)) GO TO 55
       IF(RM(I) .LT. TT(6)) GO TO 56
       IF(RM(I) .LT. TT(7)) GO TO 57
       IF(RM(I) .LT. TT(8)) GO TO 58
       IF(RM(I) .LT. TT(9)) GO TO 59
       IF(RM(I) .LT. TT(10)) GO TO 60
       IF(RM(I) .LT. TT(11)) GO TO 61
       IF(RM(I) .LT. TT(12)) GO TO 62
       IF(RM(I) .LT. TT(13)) GO TO 63
       IF(RM(I) .LT. TT(14)) GO TO 64
       IF(RM(I) .LT. TT(15)) GO TO 65
       WRITE(6,307)  I, RM(I)
  307  FORMAT(1X,'DROP NO.=',I10,3X,'RM=',F12.4)
```

```
C       AUXILIARY STAGE SHUT OFF
        ISS2=2
        NSS2=2
        GO TO 67
   51   NUMB(1)=NUMB(1)+1
        GO TO 67
   52   NUMB(2)=NUMB(2)+1
        GO TO 67
   53   NUMB(3)=NUMB(3)+1
        GO TO 67
   54   NUMB(4)=NUMB(4)+1
        GO TO 67
   55   NUMB(5)=NUMB(5)+1
        GO TO 67
   56   NUMB(6)=NUMB(6)+1
        GO TO 67
   57   NUMB(7)=NUMB(7)+1
        GO TO 67
   58   NUMB(8)=NUMB(8)+1
        GO TO 67
   59   NUMB(9)=NUMB(9)+1
        GO TO 67
   60   NUMB(10)=NUMB(10)+1
        GO TO 67
   61   NUMB(11)=NUMB(11)+1
        GO TO 67
   62   NUMB(12)=NUMB(12)+1
        GO TO 67
   63   NUMB(13)=NUMB(13)+1
        GO TO 67
   64   NUMB(14)=NUMB(14)+1
        GO TO 67
   65   NUMB(15)=NUMB(15)+1
        GO TO 67
   67   CONTINUE
        WRITE(6,401) (SS(I), I=3,15)
```

```
 401  FORMAT(1X,'COVERED',1X,'PRIMARY',13F8.2)
      WRITE(6,308) (NUMB(I), I=1,15)
 308  FORMAT(15I8)
      RANOD=0.00
      DO 721  I=3,15
      RANOD=RANOD+NUMB(I)*SS(I)
 721  CONTINUE
      NUMBT=0
      DO 33 I=3,15
      NUMBT=NUMBT+NUMB(I)
  33  CONTINUE
      ADS=RANOD/NUMBT
      WRITE(6,306) NUMBT, ADS
 306  FORMAT(1X,'TOTAL NO. OF DROPS=',I10,5X,'AVERAGE DROP SIZE=',F10.4)
C     END OF DROP SIZE DISTRIBUTION CALCULATION
C
      DAREA=0.00
      DO 42 I=1,NN
      IF(R(I))  42,42,43
  43  DAREA=DAREA+(3.1416*R(I)*R(I))
  42  CONTINUE
      DAREAM=DAREA/(3.2808E-06*3.2808E-06)
      WRITE(6,404) DAREAM
 404  FORMAT(1X,'DAREAM=',F16.4,' SQUARE MICRONS')
      IF(MSTAGE .EQ. 1) GO TO 602
C
C      CALC. OF EFFECTIVE HEAT TRANSFERRED
      SAREA=AREA-DAREA
      HPH=(THTC1*SAREA*TSTEP*DTEMT)/3600.
      TVOL=HPH/(FDEN*HEATL)
      NR=TVOL/VPD1
      WRITE(6,704) II, NR
 704  FORMAT(6X,'II=',I8,6X,'NR=',I8)
C     END FO CALC. OF EFFECTIVE HEAT TRANSFERRED
C
C     TEST FOR NR .LT. NUMB(2)
```

```
      IF(NR .GT. NUMB(2)) GO TO 726
      GO TO 27
  726 WRITE(6,728)
  728 FORMAT(6X,'NR .GT. NUMB(2)')
      NR=NUMB(2)
   27 CONTINUE
C     END OF TEST
  602 CONTINUE
C
C     TERMINATION CRITERIA
      CAREA=NUMB(15)*AF
      PERC=CAREA/AREA
      WRITE(6,403) PERC
  403 FORMAT(1X,'PERC=',F10.4)
      JYI=II
      JII=II
C     END OF TERMINATION SHUT-OFF
C
C     LOADING THE NWSS ARRAY
      IF(AGOR .LT. 11000.0) GO TO 644
      KRU=KKV(IR)
      GO TO 645
  644 KRU=KKV(IR)-1
  645 CONTINUE
      IF(IR .EQ. 1) GO TO 621
      KRY=KKV(IR-1)
      IRY=15-(KKV(IR)-KRY)
      GO TO 622
  621 CONTINUE
      IRY=3
      KRY=KVV(IR)
  622 CONTINUE
      DO 620 I=KRY,KRU
      NWSS(I)=NWSS(I)+NUMB(IRY)
      IRY=IRY+1
      IF(IRY .EQ. 16) GO TO 623
```

```
 620  CONTINUE
 623  CONTINUE
C
C      BARE AREA CALCULATION
       IF(IR .EQ. 1) GO TO 639
       ILU=KKV(IR-1)
       GO TO 640
 639   ILU=KVV(IR)-1
 640   CONTINUE
       VALUE=WTT(ILU)*3.2808E-06
       ARE=0.0
       DO 628 I=1,NN
       IF(R(I)) 628, 628, 629
 629   IF(R(I) .LT. VALUE) GO TO 628
       ARE=ARE+(3.1416*R(I)*R(I))
 628   CONTINUE
       BARE=(AREA-ARE)/AREA
       BAREA1(II)=BARE
       WRITE(6,635) BAREA1(II)
 635   FORMAT(6X,'BAREA1(II)=',F10.4)
       IF(BAREA1(II) .LT. 0.0) GO TO 89
       IF(AGOR .LT. 3.20) GO TO 646
       IF(AGOR .GT. 9000.0) GO TO 646
       IF(PERC .GT. 0.20) GO TO 674
       GO TO 647
 646   IF(NSS2 .EQ. 2) GO TO 674
 647   CONTINUE
       IF(AGOR .LT. 11000.0 .AND. ISS2 .EQ. 2) GO TO 674
    3  CONTINUE
C
 674   CONTINUE
C      SPECIAL ARRANGEMENTS FOR SDEN .EQ. 10**10
       IF(IR .EQ. 1 .AND. II .EQ. 1) GO TO 650
       JII=(JII/2)*2
       II=JII
       GO TO 651
```

```
 650  CONTINUE
 651  CONTINUE
      TTIME(IR)=TIME1(II)
      AAREA(IR)=AREA
C
C     CALC. OF THE TIME AVERAGE OF NO. OF DROPS PER CM**2 FOR A STAGE
      IF(IR .EQ. 1) GO TO 626
      MY=JYI-2
      MYL=3
      GO TO 627
 626  MY=JYI
      MYL=1
 627  CONTINUE
      DO 633 I=KRY,KRU
      AWSS(I)=NWSS(I)/MY
      BWSS(I)=(AWSS(I)*1.0E+08*3.2808E-06*3.2808E-06)/AREA
 633  CONTINUE
      WRITE(6,634)
 634  FORMAT(10X,'WSS(I)',13X,'AWSS(I)',13X,'BWSS(I)')
      WRITE(6,625) (WSS(I), AWSS(I), BWSS(I), I=KRY, KRU)
 625  FORMAT(6X,F10.4,F20.4,F20.4)
C
C     TIME AVERAGING BAREA1(II)
      BBAREA(IR)=0.0
      DO 636 I=MYL,II
      BBAREA(IR)=BBAREA(IR)+BAREA1(I)
 636  CONTINUE
      BBAREA(IR)=BBAREA(IR)/MY
C     END OF TIME AVERAGING OF BAREA1(I)
C
      MSTAGE=MSTAGE+1
C     INCREASE IN SCALE, REDEFINITION OF TSTEP, THTC1, AND THTC2
      SCALE=SCALE*3.162278
      AGOR=SCALE/3.2808E-06
      IF(AGOR .GT. 11000.0) GO TO 601
C
```

```
C     MATCHING GRAHAM'S SAMPLE AREA
C     GRAHAM'S SAMPLE AREA IS 3.24 CM**2
      IF(AGOR .GT. 3200.0) GO TO 642
      GO TO 643
  642 SCALE=18000.0*3.2808E-06
  643 CONTINUE
C     END OF MATCHING GRAHAM'S SAMPLE AREA
C
      AREA=SCALE*SCALE
C     FOR SDEN .EQ. 10**10 AND II .EQ. 1 AT TERMINATION
      IF(IR .EQ. 1 .AND. II .EQ. 1) GO TO 649
      TSTEP=TIME1(II/2)
      THTC2=THTC(II)
      THTC1=THTC(II/2)
      GO TO 648
  649 CONTINUE
      THTC2=THTC(II)
      THTC1=THTC2/2.0
      TSTEP=TIME1(II)/2.0
  648 CONTINUE
C     END OF SPECIAL SET UP FOR SDEN .EQ. 10**10
C
      NR1=500
      MSCALE=SCALE/3.2808E-06
      WRITE(6,729) MSCALE, TSTEP, THTC1, THTC2
  729 FORMAT(6X,'SCALE=',I10,6X,'TSTEP=',E11.4,6X,'THTC1=',E11.4,
     16X,'THTC2=',E11.4)
      GO TO 71
  601 CONTINUE
C     INITIALIZE FACTOR ARRAY
      DO 590 I=1,10
      FACTOR(I)=0.0
  590 CONTINUE
C
C     CALCULATION OF PA ARRAY
      PA(1)=TTIME(1)/TTIME(IR)
```

```
      DO 630 I=2,IR
      PA(I)=(TTIME(I)-TTIME(I-1))/TTIME(IR)
  630 CONTINUE
      WRITE(6,638)
  638 FORMAT(5X,'I',11X,'PA(I)')
      WRITE(6,637) (I, PA(I), I=1,IR)
  637 FORMAT(I6,6X,F10.4)
C     CALCULATION OF FACTOR ARRAY
C
      DO 631  I=1,IR
      IB=IR+1-I
      IF(I .GT. 1) GO TO 632
      FACTOR(IB)=PA(IB)
      GO TO 631
  632 FACTOR(IB)=PA(IB)+BBAREA(IB+1)*FACTOR(IB+1)
  631 CONTINUE
      WRITE(6,617)
  617 FORMAT(9X,'I',12X,'AAREA(I)',11X,'BBAREA(I)',12X,'TTIME(I)')
      WRITE(6,607) (I, AAREA(I), BBAREA(I), TTIME(I), I=1,IR)
  607 FORMAT(I10,10X,E10.4,10X,E10.4,10X,E10.4)
      WRITE(6,616)
  616 FORMAT(9X,'I',11X,'FACTOR(I)')
      WRITE(6,615) (I, FACTOR(I), I=1,IR)
  615 FORMAT(I10,F20.6)
C
C     CONVERSION OF NWSS ARRAY INTO ACUTAL NUMBER OF DROPS PER CM**2
C     INITIALIZE NDELN ARRAY
      DO 591 I=1,35
      DELN(I)=0.0
  591 CONTINUE
C
C     CALCULATION OF DELN ARRAY
      LOS=1
      KRV=KVV(LOS)
  593 CONTINUE
      KRW=KKV(LOS)
```

```
      DO 592 I=KRV, KRW
      DELN(I)=FACTOR(LOS)*BWSS(I)
  592 CONTINUE
      KRV=KRW+1
      LOS=LOS+1
      IF(LOS .GT. IR) GO TO 594
      GO TO 593
  594 CONTINUE
C     END OF CLACULATION OF NDELN ARRAY VALUES
C
C     CLACULATION OF HEAT TRANSFER COEFFICIENT FROM THE DROP DISTRIBUTION
      DO 596 I=1,35
      WSSF(I)=WSS(I)*3.2808E-06
  596 CONTINUE
      THTCD=0.0
      ARL=20.0*3.1416*THCON*HTCI
      ARM=(2.0*THCON)/(HTCI*HTCI)+RMIN/HTCI
      DO 597  I=1,35
      ARN=(2.0*THCON+1.2*HTCI*WSSF(I))/(2.0*THCON+0.8*HTCI*WSSF(I))
      THTCD=THTCD+(ARL*(DELN(I)/0.1076E-02)*(0.4*(WSSF(I)/HTCI)
     1-ARM*ALOG(ARN)))
      HTCD(I)=THTCD
  597 CONTINUE
      WRITE(6,614)
  614 FORMAT(5X,'I',8X,'WSS(I)',17X,'BWSS(I)',17X,'DELN(I)',8X,'HTCD(I)
     1')
      WRITE(6,613) (I,WSS(I), BWSS(I), DELN(I), HTCD(I), I=1,35)
  613 FORMAT(I6,4X,F10.4,4X,F20.4,4X,F20.4,4X,E11.4)
      WRITE(6,598) THTCD
  598 FORMAT(6X,'THTCD=',E11.4,' BTUS PER FT.**2 HR. DEG.')
   89 CALL EXIT
      END
```

```
C
C       IBM SCIENTIFIC SUBROUTINE RANDU
C       THIS SUBROUTINE IS A RANDOM NUMBER GENERATOR
        SUBROUTINE RANDU(IX,IY,YFL)
        IY=IX*65539
        IF(IY)5,6,6
    5   IY=IY+2147483647+1
    6   YFL=IY
        YFL=YFL*.4656613E-9
        RETURN
        END
```

APPENDIX E

DESCRIPTION OF OUTPUT

This appendix is added to assist a possible future user of the program. The output will be categorized and discussed in the order which it appears.

1. The input variables defined in Appendix C are written as the first output. These units are given. Next, the result of a calculation of minimum drop radius and the variables for the drop growth model are written out. This information is contained in the first twelve lines of output.

2. Each time step has ten lines of output. The time step output variables are written below as they appear.

"HTC" is the instantaneous heat transfer coefficient for the time step in BTU/HR FT^2°F.

"TIME" is the simulation clock time in seconds.

"THTC" is the time averaged heat transfer coefficient.

"COALESCENCE COUNTER" is the number of coalescences which occurred during the time step.

Distribution categories are listed. "COVERED" implies that the drop site is blanketed or covered. "PRIMARY" implies that a drop site is uncovered. Other distribution categories are listed as drop radii in microns. A radius category is defined by a radius differential of

forty percent. Beneath the distribution categories, the numbers of each kind is listed.

"TOTAL NO. OF DROPS" is simply the total number of drops on the stage surface at the end of the coalescence routine.

"AVERAGE DROP SIZE" is the average size of a drop existing on the surface at the end of the coalescence routine.

"DAREAM" is the amount of area covered by drops after coalescence and has the units of square microns.

"PERC" is the percentage of the stage area covered by drops of the category which can cause termination of the stage.

"BAREAM" is the amount of bare area in square microns after coalescence. This variable is the last of the time step variables.

3. The third major kind of output data described is the start up procedure between the stages. The variables will be listed and described as they appear.

"SCALE" is the dimension of the side of the next stage square in microns.

"TSTEP" is the time step for the next stage in seconds.

"THTC1 and THTC2" are the time averaged heat transfer coefficients obtained from the pervious stage result. The start up iteration matches these values for the next stage.

Iteration sequence usually consist of several lines on which the iteration variables repeated. "LC" is the number of the iteration trial. "NR1" is the number of drops to be located on the stage area for the first time step. "RMM1" is the radius of uniform drops produced on the bare area. "HCK" is a comparison of the time averaged heat transfer coefficients for the two consecutive stages at the second time step of the later stage. "RMM12" is the radius in microns which the uniform drops obtain after growing for one time step. The iteration ends when the "HCK" value is within acceptable tolerances. The number of sites on the uniformly spaced stage area is indicated by the variable "NNLT". The appearance of this variable implies the completion of the start up process.

4. At the end of the last stage, the output for the last time step contains the time averaged heat transfer coefficient for the entire process (THTC). The time to produce a drop of the departing size is listed as the variable "TIME". Also the size and number of departing drops are listed.

5. The last significant output is an array containing the information of the drop distribution. The output variables are described as they appear.

"WSS(I)" values are the radius categories of the drop distribution.

"BWSS(I)" values are the time average distribution of drops resulting from the separate stage calculations. The units are drops per square centimeter.

"DELN(I)" values are the time average drop distribution for the complete simulation cycle and have units of number of drops per square centimeters.

"HTCD(I)" is the cumulative heat transfer coefficient for all drops of a given size ("WSS(I)") or smaller.

"THTCD" is the time averaged heat transfer coefficient for the entire cycle and is calculated from the distribution of drops. This output variable is the last of the program.

APPENDIX F

MAXIMUM THEORETICAL HEAT TRANSFER COEFFICIENT

An estimate of the maximum theoretical heat transfer coefficient can be made from the maximum rate of heat transfer through a single drop. Starting with an expression for the heat flux through a single, drop, the maximum theoretical coefficient is derived below.

$$Q = \rho H_{fg} \frac{dV}{dt} \tag{F.1}$$

For a hemispherical drop,

$$\frac{dV}{dt} = 2\pi r^2 \frac{dr}{dt} \tag{F.2}$$

The heat transfer coefficient is defined as follows

$$h = \frac{Q}{A} \frac{1}{\Delta T} \tag{F.3}$$

Substituting equation (F.3) into equation (F.4),

$$h = \frac{\rho H_{fg}}{\Delta T\ A} 2\pi r^2 \frac{dr}{dt} \tag{F.4}$$

The area of the base of the drop is πr^2.

$$h = \frac{\rho H_{fg}}{\Delta T} 2\frac{dr}{dt} \tag{F.5}$$

Substituting in dD/dt for 2dr/dt,

$$h = \frac{\rho H_{fg}}{\Delta T} \frac{dD}{dt} \tag{F.6}$$

The expression (F.6) for the heat transfer coefficient becomes a maximum when the drop growth rate variable (dD/dt) obtains its maximum value. Drop growth rate is defined by equation (A.13) in Appendix A. Finally, the maximum theoretical heat transfer coefficient is expressed below as equation (F.7).

$$h_{max} = \frac{\rho H_{fg}}{\Delta T} \left(\frac{dD}{dt}\right)_{max} \qquad (F.7)$$

APPENDIX G

DERIVATION OF MAXIMUM NUCLEATION SITE DENSITY

To ensure that the site densities used in this study were realistic, a derivation of a theoretical maximum density was made. It should be noted that the theoretical maximum is much greater than could be attained on a real condensity surface.

Nucleation centers are assumed to be arranged in a triangular array, and the distance between centers is equal to twice the minimum drop radius (see Appendix A). For a triangular array, ninety-one percent of the condensing surface is covered if the sites are circular. An equation can be derived which gives the maximum density as a function of the temperature difference and other properties.

$$\text{Maximum Site Density} = \frac{.91}{\pi r^2} \times 10^8 \ (\text{sites/cm}^2) \tag{G.1}$$

The radius, r, is equal to the minimum drop radius in microns and is defined below.

$$r_{min} = \frac{2T_s\sigma}{H_{fg}\rho} \frac{1}{\Delta T} \tag{G.2}$$

Substituting in equation (G.2) into equation (G.1), the maximum theoretical site density as a function of the temperature difference and other properties can be obtained.

Thesis 127251
H942 Hunt
Computer simulation
of the dropwise con-
densation process.